Cardiff University

School of Engineering

MPhil Thesis

Neil Sykes

The manufacture of a prototype laser machined chromatographic separations column

June 2011

Abstract

This thesis details the experimentation and developments in the production of a novel laser machined prototype graphitic separations column utilizing an array of graphitic micro-pillars. The column was created with a 5kHz Thales femtosecond laser, a highly focussed beam from a stationary multi-element focussing lens to machine the fluidic tracks and micro-pillared array directly into a graphitic block as a single structure.

This novel HPLC column format could potentially create a much more robust separations column with respect to temperature and pressure and reduce the band broadening associated with conventional chromatographic columns because of the inhomogeneous bead packing and the influence of side walls.

The computer-aided design (CAD) was developed in Alpha-Cam and converted into code for the motion control system in order to traverse the workpiece in X and Y with an Alpha-Cam post processor.

An integrated on-chip sample injector and fluidic flow-distributor are incorporated onto the column to minimize band broadening and enable more equal fluid flow across it. Half pillars were machined into the edge of the array to minimize band broadening.

The separation column was integrated directly with the ESI probe of a Thermo Fisher Surveyor mass spectrometer. The device was tested at HPLC pressures and successfully performed without leakage. It's evaluation as a chromatographic separations column showed the repeated partial separation of two molecules. This represents the first demonstration of a micro-machined graphitic microfluidic device and it's performance in separation science.

Acknowledgements

The author would like to thank the following people for their advice, assistance and encouragement during this research.

Professor David Barrow at MetaFAB Cardiff University for his supervision and guidance

Professor Adrian Porch - Cardiff University

Dr. Oliver Castell – MetaFAB Cardiff University

Helen Giles- Cardiff University

Dr. Harald Ritchie – Thermo-Fisher

Professor Peter Myers – Liverpool University

Index

Figures

1 Introduction

High performance liquid chromatography, also referred to as high pressure liquid chromatography (HPLC), is a technique that can separate and identify a mixture of compounds in a fluid and is used in analytical chemistry.

Traditionally the analyte is dissolved in a liquid called the mobile phase, this is then pumped through a column that is densely packed with porous spherical beads. The beads have a high internal surface area. The compounds within the analyte are separated by differential retention. Each chemical species takes a different time to travel through the column; this time is related to the chemical species mass, charge and structure and is reproducible. The method has some deficiencies that reduce the reproducibility between columns and cause band broadening; these are caused by irregular packing of the beads in the column and issues where the beads meet the sidewall of the column itself. A solution to these problems could be the manufacture of an ordered column array. This thesis shows the experimental details of the manufacture and testing of an ordered pillar array manufactured in graphite using a laser.

1.1.1 Aims

The aim of this project is to manufacture a prototype high pressure liquid chromatography (HPLC) separations column using a graphite block as the stationary phase. The stationary phase and associated fluidics are directly laser machined into the graphite using the Cardiff University MetaFAB facility lasers to create separations pillars, fluidic path and flow distribution control. This in turn is encapsulated to seal the laser machined stationary phase while allowing the controlled passage of fluids into and out of the column through holes machined through the block and interfaced with micro-fluidic connectors. The assembled device is connected directly to the metaFAB Thermo Fisher HPLC to test and assess the device function.

1.1.2 Facilities

The majority of this work was completed at metaFAB which forms part of the School of Engineering at Cardiff University. The metaFAB facility houses specialist equipment which includes key equipment relevant to this project:

- The metaFAB Xtreme Laser Facility has a number of lasers specially chosen to have the ability to manufacture microfluidic circuits in optical and specialist materials. These include an Exitech M2000EF machine with both a femtosecond and 157nm laser sources located on the same platform.

- metaFAB Analytics which includes a Thermo Fisher High-Performance Liquid Chromatography Mass Spectrometer.

- metaFAB Metrology, a suite of high quality optical microscopes and a Veeco optical interference surface profiler.

1.2 Literature Review

1.2.1 Graphitic materials

Graphitic carbon experimented with as a stationary phase in liquid chromatography was initially referred to as porous glassy carbon (Gilbert et al. 1982) and then with process improvements it became known as porous graphitic carbon (Knox et.al. 1986). This porous graphitic carbon is most commonly used in a spherical particulate form that is used to pack columns. Graphitic carbon has also been used as a coating, on an existing silica or carbon stationary phase, in an attempt to improve the stationary phase mediums separation performance (Colin & Guiochon 1977).

The manufacture of porous graphitic carbon uses silica particles as a template which is impregnated with phenol and hexamine and then heated (West et al. 2010) to crosslink the polymer. This polymer is then pyrolysed at 1000℃ in Nitrogen, and the silica template is subsequently removed and the graphitisation realised with a thermal treatment at a temperature of 2340℃ in Argon. This has been a commercial process since 1988 under the trade name Hypercarb® by Thermo Electron Corporation. Since 1988 the process has been optimised and particles have been produced as small as 3µm. This allows Hypercarb to compare well with bonded silica gels with respect to chromatographic performance (Pereira 2008).

The interest in graphitic carbon as a stationary phase material is based on the physical and chemical properties of carbon; these include the ability to withstand extreme mobile phase pH conditions (10M acid through to 10M alkali) (Ross & Knox 1997), which extends the diversity of analytes that may be examined and creates a chemically robust column. Two recent reviews (Periera 2008.West et al 2010) provide an extensive analysis of porous graphitic carbon.

Spherical particles of graphitic carbon are packed into tubes to create separation columns. Due to inhomogeneities in the stationary phase packing, and through axial analyte diffusion, significant band broadening can occur

(Eikel 2007). The manufacture of highly ordered monolithic arrays of pillars, as an alternative to traditional spherical packing material, could address this issue. Computational fluid dynamics suggest that closely packed diamond shaped pillars (De Smet 2004) are likely to provide the best chromatographic separation results.

High aspect-ratio pillars have previously been manufactured by the etching of silicon (Park et al. 2003). These silicon pillars are usually coated with silicon dioxide to replicate the surface of the conventional particulate media and also reduce the inter-pillar distances left from the etching. This process, referred to as the Bosch process cannot be used on graphite because the plasma chemistry is fairly specific to silicon.

The Lab-on-a-chip approach has created interest in this field and studies in the field of chromatography have been investigated by He and Regnier (1997). Ideas within this area include the use of nano-litre samples which has both financial and environmental advantages and possibilities of the manufacture of relatively large arrays of monolithic pillars. The structures created however, are based on silicon and use a chemical etching process rather than laser micromachining.

The manufacture of synthetic moulded graphite from powders often uses a binding agent. Commonly this is a phenolic resin producing a C-polymer composite (Cunningham *2005)* that constitutes approximately 10% of the mass. The Graphite used in this work consists of particles with a grain size in the region of 10μm. Graphite is available with great variation of porosity and the binding agent has a large effect on this. Graphite is available as a C-polymer graphite with a 10% phenolic binding agent. However, the binding agent can be added at various quantities up to saturation creating a denser, much less porous substrate.

Figure 1. *A Thermosfisher Hypercarb HPLC column with a 50mm x 3mm active column and 5 µm particle size.*

1.2.2 Laser machining of Graphite

Pulsed laser ablation is ideal for the micromachining of materials as the heat affected zone is minimal compared to the very thermal CW laser methods that are not suitable for machining on the micron scale. Different machining methods have been developed for each laser type due to the wide variation of pulse duration and beam quality of emission; these methods range from high speed galvanometer scanning of a focused beam from a kHz YAG laser, to mask imaging techniques from homogenized flat-top beams from excimer lasers. Excimer lasers can also use techniques such as mask scanning that could allow a complex pattern, such as a complete separations column, to be ablated at high speed into the surface of a graphitic sample. Synchronized image scanning (SIS) is a relatively new technique *that* could directly machine

an array of upstanding columns in the surface of a graphitic sample, whilst the fluid distribution network could employ direct write techniques.

Femtosecond lasers have been shown to have the ability to produce high quality micromachining in many materials (Ostendorf et al.2002). This is due in part to the ultra-short laser pulse interaction with the material and also the non-linear absorption that allows the micromachining of materials otherwise transparent to the wavelength in use. With ultra-short pulse lengths extreme states of matter can be reached allowing unique possibilities of structural modification or material removal (Sokolowski-Tinten et al.2000).

Micromachining structures in material with femtosecond lasers is achieved by a very high peak laser intensity with relatively low pulse energy (Liu et al.1997*),* This limits the heat affected zone allowing the fabrication of micro-scale features with little or no obvious thermal damage from the laser process.

The use of femtosecond lasers for the direct manufacture of chemical separations columns in graphite is not documented but impressive aspect ratios of blind hole diameter compared to depth have been reported for silicate glasses (Shah et al.2001*),* however as the authors of this imply, this is assisted by a self focusing phenomena and it may not be possible to produce this in graphite.

1.2.3 High-performance liquid chromatography

High-performance liquid chromatography (HPLC) has many valuable applications in commercial and non-commercial fields. Improvements in the field of drug testing using HPLC, and in particular Mass Spectrometry, can be tracked through the decades with methods utilised in the performance enhancing drug testing of athletes in the Olympic Games (Hemmersbach, 2008). Similar uses extend to forensic investigations to detect and identify poisons and drugs at crime scenes (Labat et al., 2004). It is also widely used in the pharmaceutical industry for quantitative and shelf-life investigations and

equally in the food and water industries for a diverse range of applications from the detection of estrogens and phenols in water to sugar analysis.

This analysis depends on the ability to separate compounds and elements within a sample. This chemical separation in HPLC relies upon a column which separates analytes by differential retention. Essentially different compounds and elements travel at different rates through the column. The rates are known and software can analyse the mass to ascertain the chemicals contained within the assay. The relative quantity measured can also give information on the relative quantity of the analytes in the sample.

Conventional HPLC columns, as shown in Figure 1, are used for a wide range of analyte detection; these include water quality, drug and food testing.
Any chromatographic bed needs to be enclosed with an impermeable wall. This leads to a thin region close to the wall where the packing density is significantly different to the rest of the bed. The presence of this wall even if only pillar wide will give rise to a significant band broadening. Computer simulations of the packing process (Broeckhoven & Desmet. 2007) indicate it takes several particle layers before the effects of this are negligible. The packing structure in particulate packed columns is also prone to a larger scale density variation caused by an uneven distribution of the packing stresses; this is likely to have more effect than side wall issues as it leads to a warping of the eluting bands causing band broadening.

1.3 Manufacture of a prototype column

1.3.1 Key equipment

1.3.1.1 Exitech M2000EF

Figure 2. *Front view of the Exitech M2000EF laser workstation showing operator console and load doors.*

The Exitech M2000EF Laser micromachining workstation (figure 2) was manufactured by Exitech Limited in 2005. The machine houses two independent lasers which can both work on the same workpiece albeit at different times; these are a Lambda Physik Excimer Laser specially adapted to give an output wavelength of 157nm with pulse lengths in the region of 20nsec and a Thales Femtosecond Laser which gives extremely short pulses of approx 150fs at 790nm.

The 157nm Excimer laser was manufactured by Lambda Physik (now part of Coherent Inc.) and is suitable for machining by mask imaging in a large range

of materials including fused silica and other optical materials that are otherwise difficult to machine with lasers due to their optical transmission range. The laser light is generated by a high voltage discharge through a gas mix of Fluorine and Neon at a pulse rate of up to 200Hz. The wavelength of 157nm is too short a wavelength to travel through air, and therefore, all of the beam tubing is purged with high purity Nitrogen. The Oxygen content is monitored and the laser is only used when the beam lines have <50ppm of O_2 present otherwise the ozone created when the 157nm light is absorbed in the oxygen can damage the laser machine optics.

The beam shaping optics of the machine are manufactured from Calcium Fluoride and a modified fused silica (which is >80% transmitting at this wavelength). These optics shape the beam to give a flat-topped uniform laser beam profile at the mask plane using fly's eye homogenisers. They achieve this by splitting the beam into 36 parts and overlapping them on themselves. The beam at the mask plane would then go through a mask. The mask would be normally manufactured out of metal and the pattern on the mask would be imaged onto the workpiece using a reflective lens with a demagnification of X25. Details of the optical components are shown in figure 3.

The optical system incorporates a backlit imaged mask for the 157nm laser system; this allows the visualisation of the mask image on the workpiece with cameras and is a valuable alignment and focussing aid. The stages are placed outside the Nitrogen environment and transmission to the workpiece is achieved by bleeding the purge gas out of the beam lines through the lens itself. The lens has a nose cone mounted on it, which bleeds the Nitrogen over the sample and effectively allows the laser radiation to reach the workpiece without being attenuated through absorption in air.

The 157nm laser has not been selected for these trials as the mask system is static and therefore the only way to machine a chromatographic column into graphite would be to use a tightly focussed spot. The machining of a column is not practical at this stage on the Exitech machine with this laser. Generating a focussed spot would be highly inefficient optically and would lead to extended process times which would extend beyond a gas fill lifetime causing process

defects as a result. However, possibilities do exist for this laser using mask projection techniques. This would require a mask to be manufactured with a series of non transparent squares (the pillars) with transmitting lines in between the pillars. This would allow the micromachining of multiple consecutive streets thereby creating the pillar structures. This requires the manufacture of a suitable mask; the mask blank needs to be transmissive at 157nm and obtaining suitable materials has proved difficult and expensive (McClay & Mcintyre 1999)

The Thales Femtosecond laser has suitable characteristics for the machining of a separations column. The laser has a pulse rate of 5kHz and uses a focussed spot to machine rather than mask imaging. This focussed spot is static and the workpiece is manipulated in X and Y to write the column and interfacing fluidics into the graphite. Although the laser is only capable of just over 1 watt of average power the laser spot size at the workpiece can be just a few microns giving extremely high energy densities even at low power settings. For example, a power setting of 0.04W gives in excess of $100J/cm^2$/pulse over a 3µm diameter which is a very high energy density, capable of machining most, if not all materials. Details of the femtosecond laser optical components are shown in figure 3.

Due to the pattern complexity, it is not feasible to directly write this in stage code. There are a number of machine based CAD programs available that allow translation from drawing to machine code. Alphacam® allows the visual design of complex patterns to be translated with a post processor to machine code (“G Code”) suitable for the XY stage sets; this also gates the laser directly, effectively turning it on and off as required.

The femtosecond laser is named as such due to its pulse length, each pulse being in the region of 150fs. Adjustments can be made to the laser to change the pulse length and checked with an autocorrelator to aid adjustment.

The workpiece is controlled with an Aerotech Inc. U500PCI controller which in turn controls 4 BA20-320 amplifiers supplying power to the 4 main machine axis, X and Y for linear motion, Z for vertical (focus) and U for rotation for

alignment. The machine has an XY spatial resolution of 100nm. The X and Y stages use linear motors and encoders which give high levels of repeatability of ±1µm in a temperature controlled environment.

An extract nozzle placed near the machining point is connected to a filtered fume extract system. The filtered gas is then released within the machine enclosure. The machine enclosure is also extracted and filtered before being released to the environment.

The focus lens used for femtosecond laser during these trials was a 0.4NA X40 standard working distance microscope objective.

The lasers are housed in a class 1 safety enclosure with interlocked doors and covers and a viewing window designed to be laser safe at 790nm and 157nm.

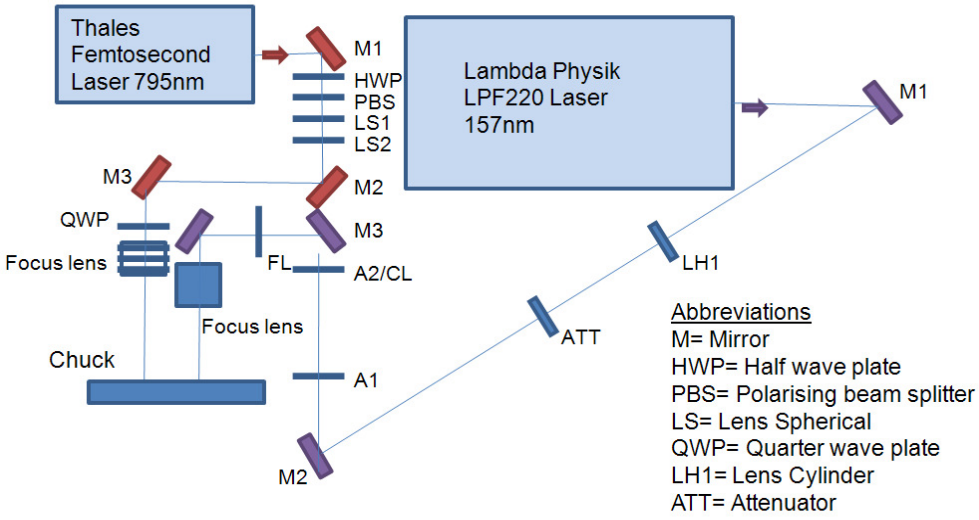

Figure 3. A schematic of the Exitech M2000EF optical system

1.3.1.2 Thermo-Fisher HPLC

The Thermo Fisher HPLC-MS is a common tool in pharmaceutical laboratories featuring a number of methods for analysing the contents of liquids and providing quantitive data.

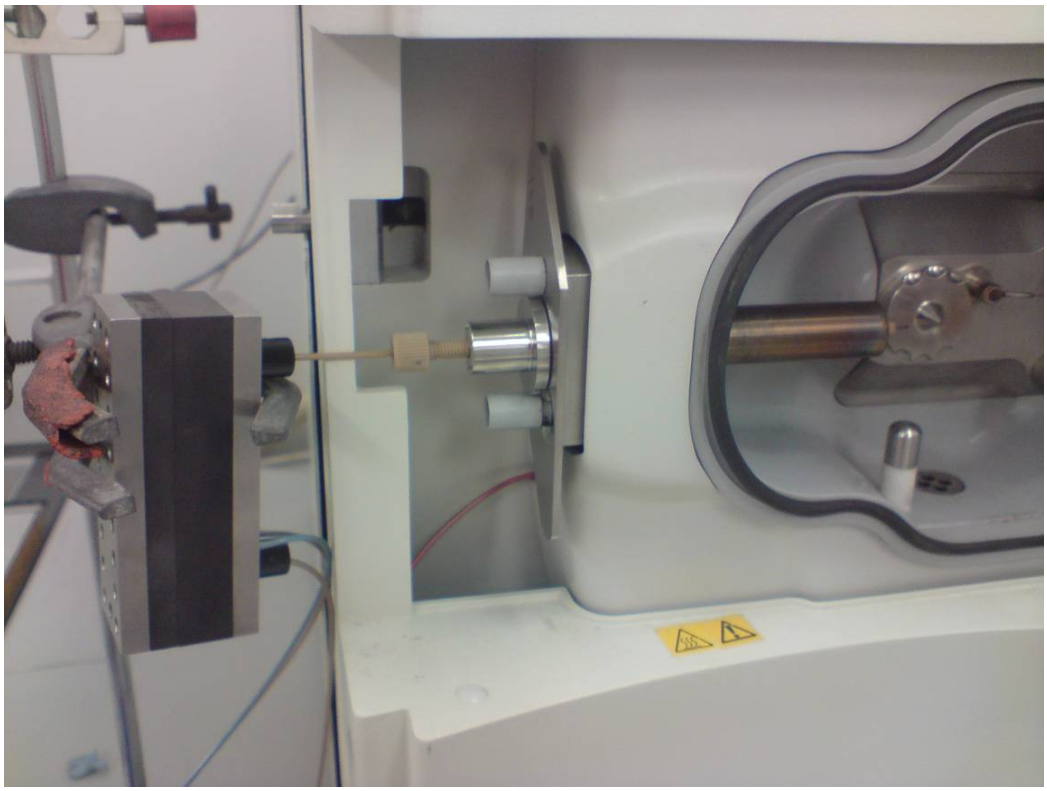

Figure 4. *The components of the Electro-spray Ionisation components integrated with a phase 2 Prototype Separations Column.*

The particular detector of interest on this equipment is the Surveyor™ MSQ™ MS detector which uses Atmospheric Pressure Ionisation and Mass Spectrometry. This sensitive instrument, shown in figures 4 and 5 allows the selective detection of organic molecules at very low analyte levels i.e sensitivity of fg to pg.

The sample is introduced into a column where separation occurs between the analytes. The sample is then ionised and passed through a mass analyser and collected at a detector. The signal from the detector is stored and the mass and time data is displayed on the control computer. Nitrogen is used both as a nebulising gas and as a sheath gas to aid ion evaporation.

Low molecular weight compounds are not normally cracked by this method so for these the measured mass is that of the full compound ± 1 proton, dependent on ionisation. This simplifies detection. At higher voltages some fragmentation can occur. To aid identification, lists detailing common fragments are available.

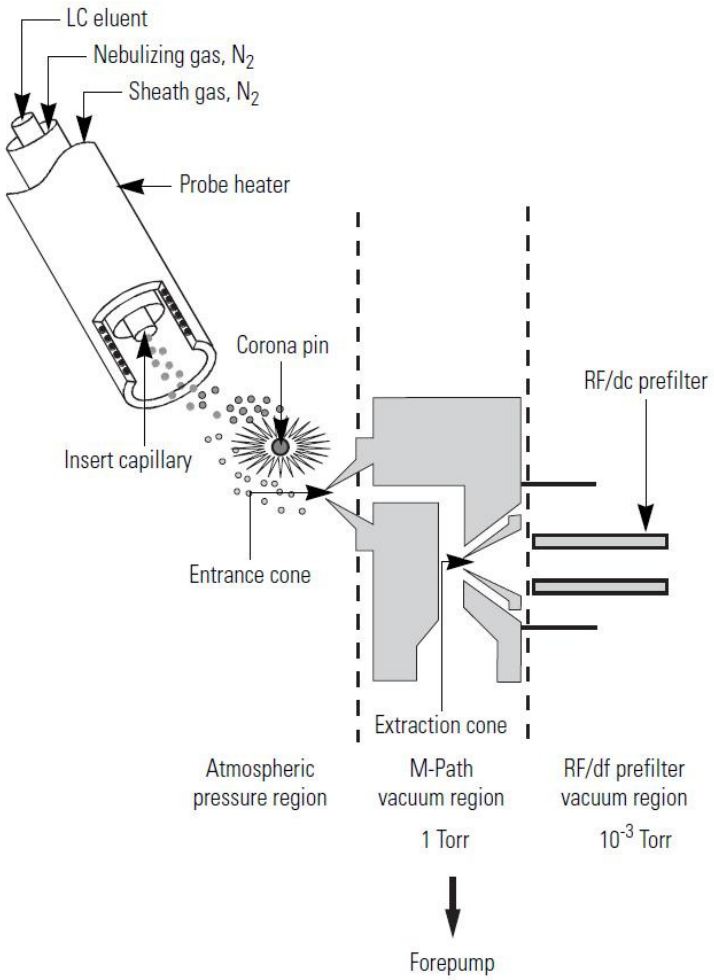

Figure 5. *Schematic showing the Electro-Spray Ionisation (ESI) source on the Surveyor MSQ including principal components and pressure ranges. Source, Thermofinnigan MSQ manual.*

1.3.2 Design considerations

The test column is expected to be operated at pressures up to 500psi. It is necessary to use materials that will reliably operate at these pressures. This is relatively easy with respect to utilising standard high pressure miniature fittings such as those already used in HPLC. The column material has to interface with these. The design in this case is to be conservative and does not aim at miniaturisation, but to manufacture a highly serviceable, robust device.

As with all HPLC devices, fluidic interfacing frequently increases the band broadening effect associated with Poiseuille flow. Bends and interfaces with interconnecting tubing , which can cause a variation in fluid speed and eddy currents can have an equally profound effect. The test column was placed as close as was reasonably possible to the detector with a minimum of bends and joints to lessen these effects.

1.3.2.1 Dimensions

The graphite material dimensions that have been selected for these tests were 76mm (3”) x 25mm (1”). This size was offered as standard from the graphite supplier (graphitestore.com, Inc) and is also the same size as a standard microscope slide. Inexpensive microscope slides were used to pre-check column patterns, alignment and laser offsets in preliminary laser micromachining trials.

1.3.2.2 Column and Fluidic Interface Material Choice

Graphite was procured from www.graphitestore.com who stock a large range of graphite materials. The graphite was described as high density, superfine

isomoulded with a ground finish and manufactured with 10µm particles. Two thicknesses were obtained; 6mm thick blocks for the laser machined stationary phase (column) substrate and 12mm thick blocks were selected for the fluidic interface substrate as it was required to be drilled and then tapped with an M6 thread to receive the miniature PEEK fluidic connector. Using a 12mm thick block would lessen the chance of the graphite breaking whilst tightening the flangeless PEEK nut.

1.3.2.3 Fluidic Interface

Initial tests required inlet and outlet tubing to be connected through the 12mm graphic block. Tests were conducted to ensure the column could withstand pressures up to 500psi without leaking from either the fluidic joints or the compression seal.

Interfacing with standard micro-fluidic tubing is required and Upchurch Scientific nuts and ferrules were used (flangeless nuts P-207X, 1/16” ferrules P-200X). The interface of the 12mm thick graphite block was machined with the inlet and outlet holes 50mm apart, 25mm from the centre of the block. These were drilled through with 1/16” diameter to match the tubing OD and then drilled from the outside at 5mm diameter to a depth of 8-9mm and then tapped M6 to accommodating the flangeless nuts. The flangeless nuts require a flat, clean base to the hole and consideration to this was made prior to tapping the hole M6.

Graphite gives a very good surface finish using conventional workshop tools and sealing issues were not encountered once the nut was tightened. The tubing was pushed into the hole until it reached the other side and then retracted very slightly just to ensure that it did not make a direct seal on to the 6mm thick block when it was applied. After initial leaks were found to occur at the inlet port the, the M6 flangeless nuts were progressively tightened. Initial fears of graphite fracture appeared to be unfounded and no failures were encountered.

1.3.3 Graphite to Graphite Sealing methods

The column was required to withstand pressures in excess of 500psi (35 bars). Therefore finding a suitable sealing method was considered essential. Compression was selected as the primary method as this would provide the ability to dismantle and examine the device after an experimental run and then reassemble and re-use all or some of the components. This proved valuable as the laser column machining process time was approximately 18 hours, so fabricating the column was very time consuming and hence relatively expensive.

1.3.3.1 Compression sealing of the column to the fluidic interface block

Compression sealing requires a high quality surface finish. The supplied graphite seemed very flat but the surface finish was poor. There was visible banding due to the grinding process and optical microscope inspection suggested a modulation between grinding bands of 0.8 -1.2µm. Therefore, the substrate was expected to require polishing to ensure a good quality seal. This polishing process was developed as required.

1.4 Phase One

1.4.1 Leak testing

Stainless steel blocks were manufactured to allow the test column to be held within the jaws of a vice. These blocks were ground flat with a standard workshop surface grinder on the surfaces which had direct contact with the test column. The contact faces were also cleaned carefully before assembly to minimise the risk of debris which could damage the test column when pressure was applied. Tissue paper was used between the rough vice jaws (figure 6) and the stainless blocks to help prevent damage to the chuck and the stainless steel blocks. The vice used was a standard engineers bench vice which was not fixed to the bench surface and as a result limited the pressure applied as the vice had to be held with one hand whilst tightening the vice with the other.

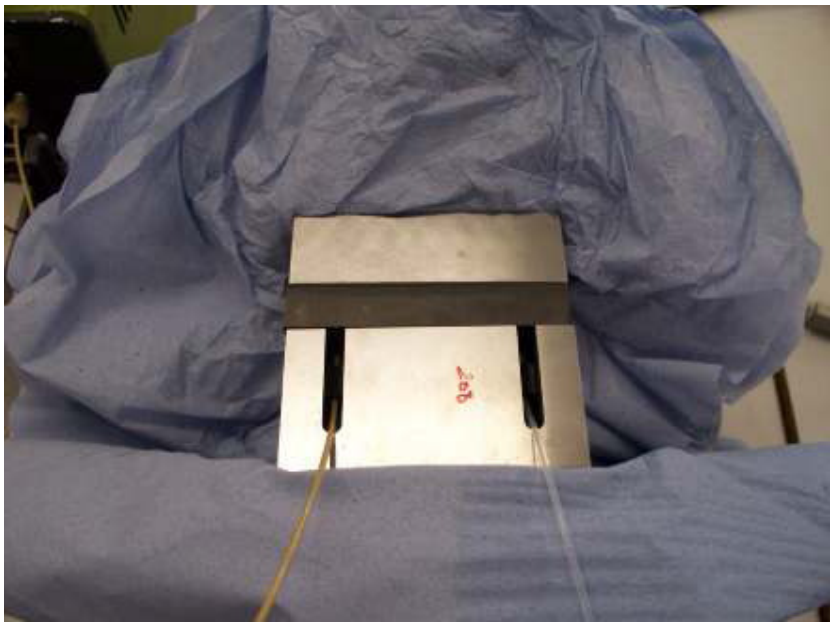

Figure 6. *The ground metal plates used to enable the test column to be held within the jaws of a standard engineering vice. The slots allow the inlet and outlet tube to connect to the test column; a recess inside protected the interface fittings.*

The ability to be able to pump fluid through the test column was essential to its operation. To ensure that the sealing method was adequate, a series of fluid pumping tests were performed using a KD Scientific syringe pump.

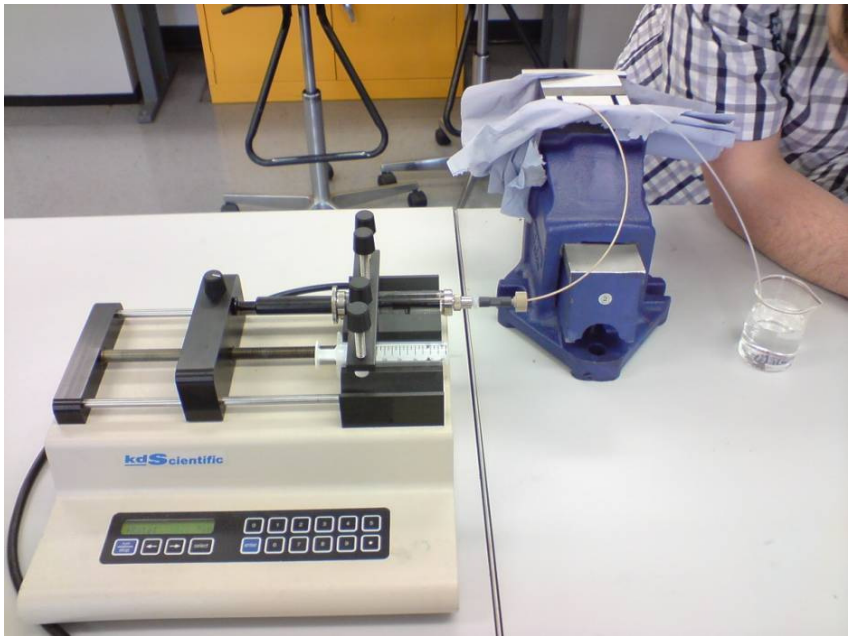

Figure 7. *Experimental set up showing the KD Scientific syringe pump with syringe connected to the inlet of the test column. The outlet tubing was connected to a collection measuring beaker where the output could be observed.*

Initial runs used a series of laser machined tracks machined into the 6mm block in positions to coincide with the inlet/outlet (figure 7). The vice jaws were tightened on each successive run and ultimately tightened to a high level. No measurement data for pressure applied was available for these initial tests.

Runs 1 through 7 conditions

The initial tests were run with the following Femtosecond Laser machined fluidic geometry:60 parallel, straight ducts, length 50mm, width 18 µm and depth 31 µm.

Laser and process settings were: Power 0.4W, Feed rate 100mm/min, Triplet lens and a single laser pass.

6 concentric circles provided feeder channels for inlet/outlet fluidic interfacing as shown in figure 8 to ensure alignment of inlet/outlet tubing with a machined channel. The inlet/outlet section was machined twice to give a greater

machining depth resulting in a depth of 70µm. The outside circle has a diameter of 3 mm.

This column design at this stage was a temporary solution and offers only parallel grooves for leak testing and needed to be redesigned for a separations device.

Leak test graphite plate ID 110608#1 was used without washing or surface cleaning or polishing.

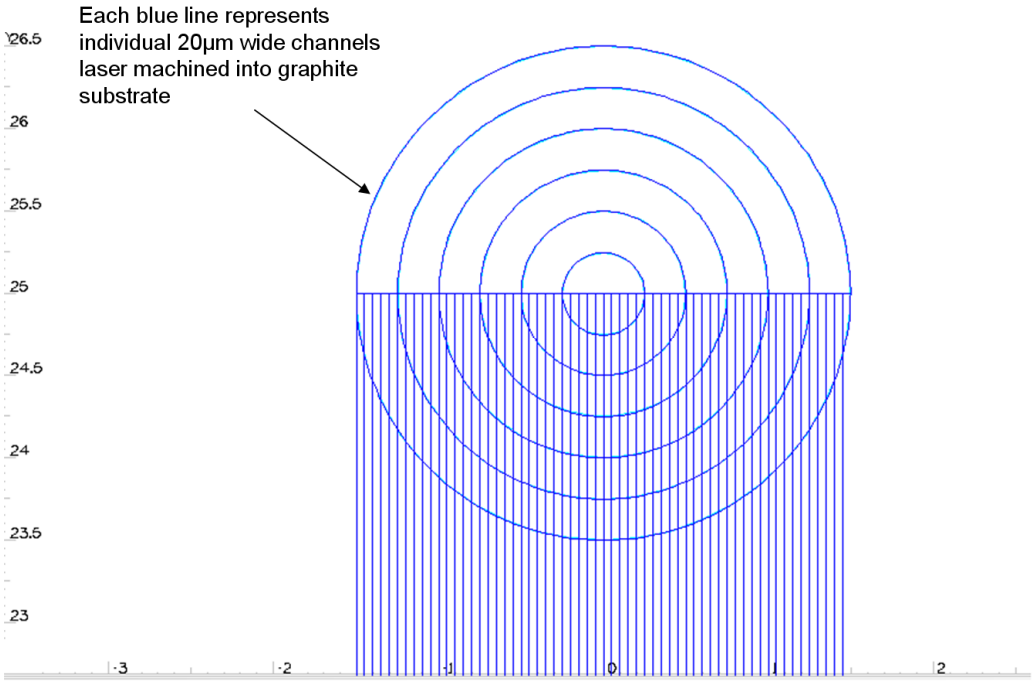

Figure 8. *The CAD data at one end of the laser machined column for the test runs 1 to 7; this was machined into the graphite surface using the femtosecond laser. The blue lines and circles are individual passes of the focussed laser beam and represent the areas machined on the graphite plate ID 110608#1.*

Fluid Supply:
Using the KD Scientific syringe pump as shown in figure 7, a number of plastic syringes were trialled and all failed through deformation of structure or failure of the seal. The Scientific Glass Engineering (SGE) glass syringes were the only ones tested that were able to take the full pressure applied by the syringe pump without failure. Using the syringe pump to deliver such pressures was considered as particularly hazardous and protective eyewear was worn at all times whilst the syringe was pressurised. Initial tests with de-ionised water utilised 10 ml glass syringes (SGE) with 6cm graduation. The adaptor used was a female luer to 10/32 finger tight screw (male) and an Upchurch PEEK union, 10/32 finger tight screw (male) + ferrule.

Flow Rates / Syringe Driver Settings:
A 15 mm diameter syringe was used at flow rates 4.8 ml/hr and 10 ml/hr (0.08 ml/min and 0.1667 ml/min respectively). The syringe diameter was calculated as 14.57mm, and therefore was delivered 94.3% of the stated flow rate. A validation check was made with fluid flow through a 40 cm length of tubing with a 500 µm internal diameter. At a flow rate of 10ml/hr (0.1667 ml/min) 0.5 ml was collected in 2ml ependorf tube in 3 min 25 s (205s) equating to a flow rate of 0.1463 ml/min. This was slightly less (93%) than the expected rate of 0.1572 ml/min.

1.4.1.1 Run 1

The initial flow rate was set to 0.08 ml/min. The outlet tubing was placed in a beaker of water and air bubbles were observed to slowly develop at the tubing outlet as air clears from the device/tubing (figure 9). The flow rate was then increased to 0.1667 ml/min to reduce the time required to clear the air. After several minutes water was observed to be leaking at the fluidic inlet in significant quantities due to conservative initial tightening of the nut. The run was stopped and the device was dried using dry clean compressed air.

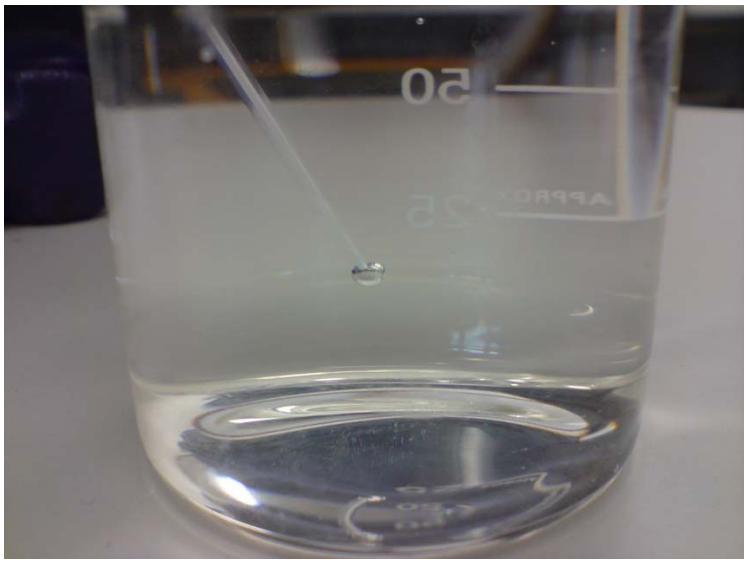

Figure 9.The clearance of air from the device upon the start of pumping.

1.4.1.2 Run 2

The Inlet connector was tightened and additional compression applied by the vice. At a flow rate of 0.1667 ml/min, leaking was still detected at the inlet and a small volume of water was observed to leak at the device interface at the inlet end of device (figure 10).The run was stopped, the device was dismantled and dried using dry, clean compressed air.

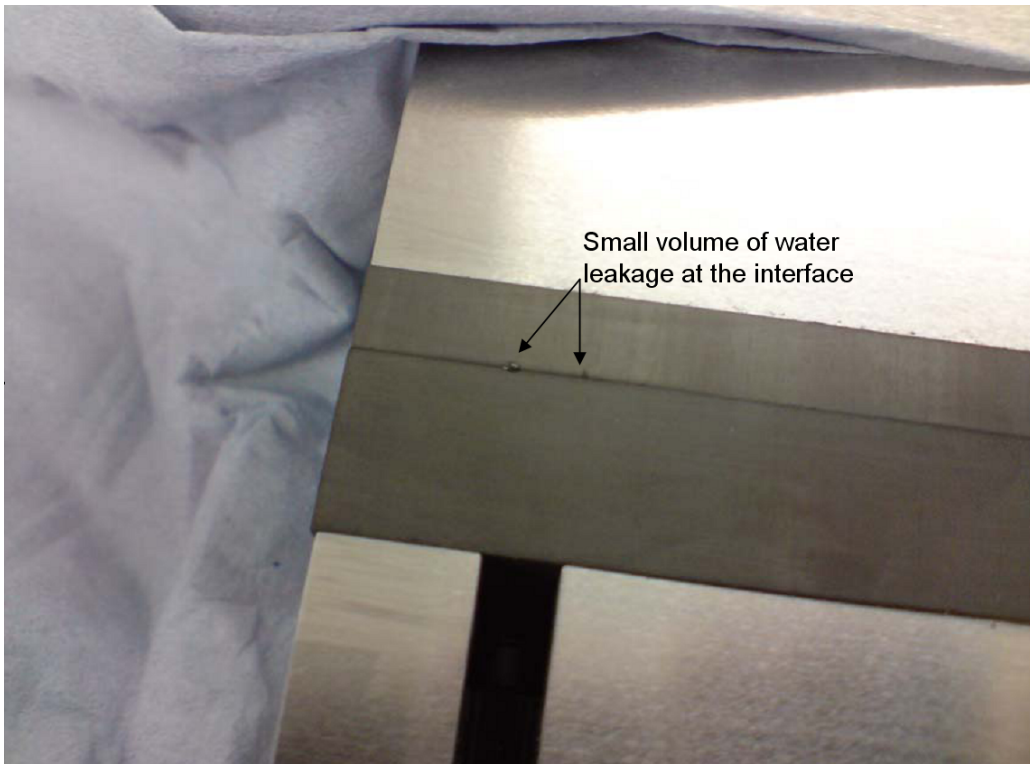

Figure 10. A small volume of water leakage at graphite-graphite interface.

1.4.1.3 Run 3

The inlet connector was tightened and additional compression applied by the vice. Using a flow of 0.1667 ml/min, water commenced flowing through the device and out of the outlet tubing. 0.5 ml was collected in 8 min 40s (520 s). The output of 0.0577 ml/min was equivalent to 39% of the flow into the device (compared to measured collected volume in unrestricted flow). The device was found to be still leaking at the inlet connector and a small volume of water observed to leak at the device interface at the inlet end of device. The run was stopped and the device dismantled and dried as before.

1.4.1.4 Run 4

The Inlet connector was tightened further and additional compression applied by tightening the vice. Again, using a flow rate of 0.1667 ml/min. the migration of an air/water interface (bubble) in the outlet tubing was measured. An air

bubble travelled 18.5 cm in 26 seconds; giving an approximate initial flow rate through the device of 0.0833 ml/min. The leak at the fluidic inlet had evidently stopped, although leakages were still observed at the graphite interface. 0.5 ml of water was collected in 5 min 8s (308 s), representing an output of 0.0974 ml/min or 67% of the input.

1.4.1.5 Run 5

Further additional compression was applied by the vice. Using a flow rate of 0.1667 ml/min, 0.5 ml of water was collected in 4 min 46s (286 s), representing an output of 0.1049 ml/min (72%). Figure 11 shows the quantity of fluid that had leaked at the graphite interface at the end of the collection time.

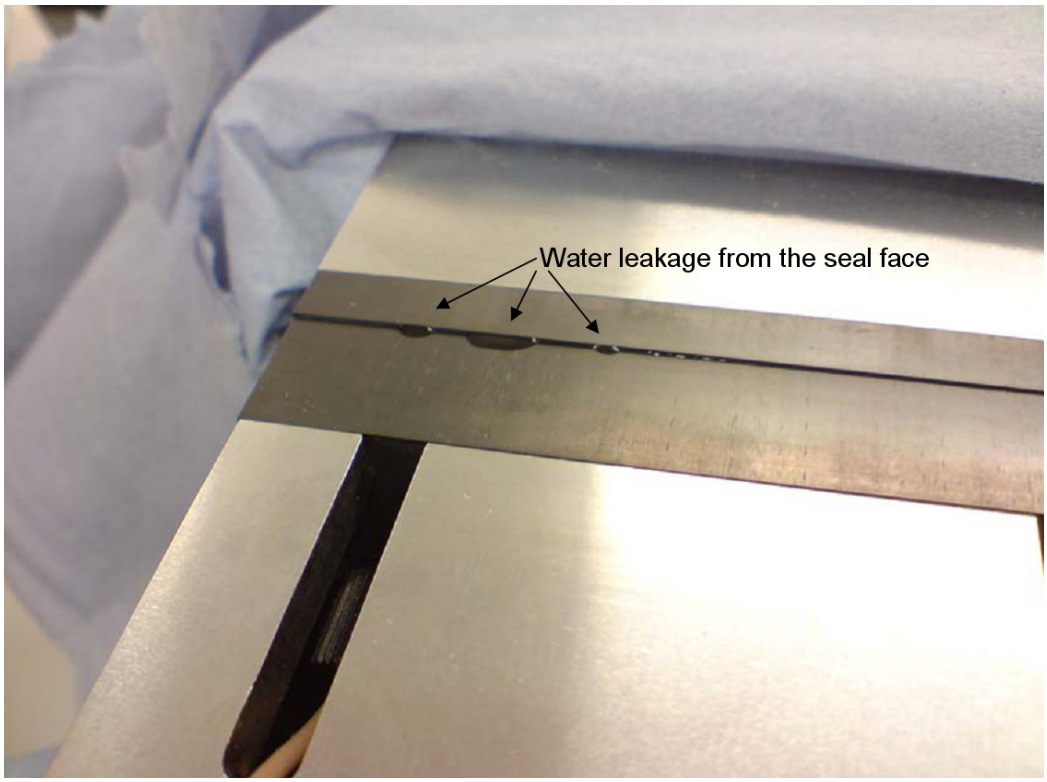

Figure 11. *Water leakage from the graphite seal face at the end of Run 5.*

1.4.1.6 Run 6

Additional compression was applied by the vice which was tightened to near the maximum possible with one hand restraining and other holding the vice. Using a flow rate set to 0.1667 ml/min. 0.5 ml of water was collected in 4 min 47s (287 s), representing a flow rate of 0.1045 ml/min (71%). It was concluded that the device may well have been at the limit of the compression seal using this method and that the continued leakage may be have been due to differences in surface height (~1 µm) resulting from the ground finish. When the device was dismantled (figure 12), graphitic particles were observed to be floating in the aqueous film on substrate surface, perhaps due to dislodged laser machining debris. The device was dried before polishing tests were conducted in an attempt to reduce surface height irregularities.

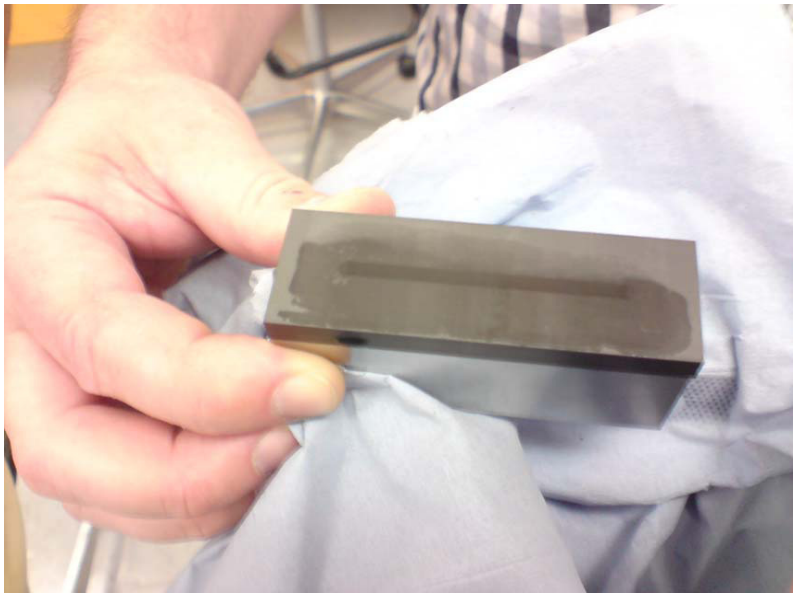

Figure 12. *The water film on the graphite substrate surface after run 6.*

1.4.1.7 Preliminary Polishing

Buehler Metadi diamond suspension ¼ micron water base (no. 40-6529) was used to hand polish both substrate halves (110608#1 and fluidic interfacing lid). The polishing method in this case utilised a polishing pad and the graphite

was polished with a figure of eight motion. The substrates were rinsed with water and dried before re-testing. The finish achieved was good with the exception of some surface scratches at various angles.

1.4.1.8 Run 7

The device was reconstructed and compression sealed with similar vice tightening as detailed in run 6 and then used with the same input flow rates. The syringe driver was unable to pump after one minute due to the gear thread slipping indicating the limit of the syringe driver operation. It was thought that this was due to increased resistance to flow from particles (diamond and/or graphite) remaining in the fluidic channels from the polishing process. A particulate containing liquid (grey/silvery) was observed to exit the outlet tubing before the flow stopped, supporting this theory. The syringe driver was able to pump at half the nominal input flow rate (0.08335 ml/min), but device leakage occurred and the syringe driver stalled again when the flow rate was increased to the original value. Leaking water was observed to appear on the far side of device as shown in figure 13. It is not clear how or why this was occurring at this stage.

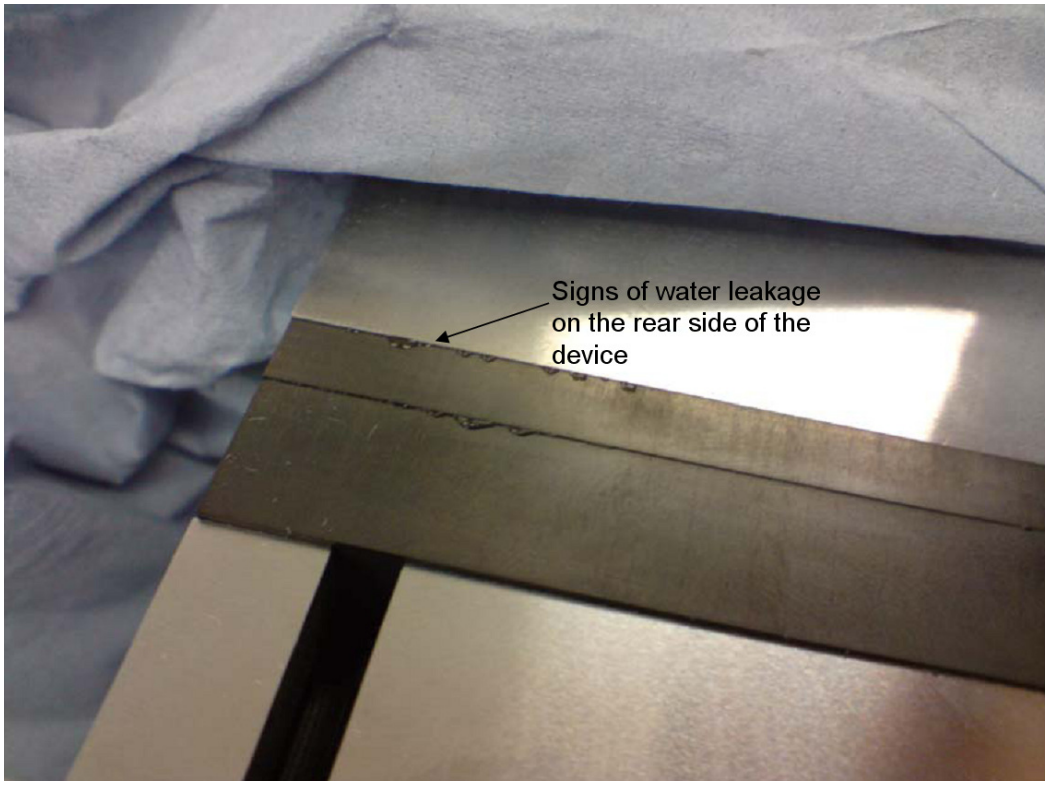

Figure 13*. Signs of water leakage on rear side of device.*

1.4.1.9 Summary of Runs 1 to 7

Summary

The delivery of water at a flow rate of 0.1463 ml/min to the microfluidic device resulted in 71% of the flow exiting the device outlet by compression sealing alone, and 29% of the water was lost elsewhere.

Flow Discrepancy

Possible reasons why the output flow rate did not equal the input flow rate include:-

- The pump required calibration; the flow level used was very close to the minimum setting level on the pump so it may have required calibration at this level.
- The flow rate was too low for the pump to give a stable output.
- Small fluidic circuit leaks occurred that are too small to detect whilst the device is clamped in the vice.
- Fluid was being absorbed within the bulk material of the graphite column.
- The syringe driver could have been partially stalling during runs.

1.4.1.10 Conclusion of Runs 1 to 7

Compression sealing with specially designed manifolds was expected to be capable of producing a leak-free seal between the two polished graphite substrates. It was also possible to interface tubing to and from the device. However, improvements were required to reduce the loss of fluid, the pumping stability and the separations column design.

Fluid loss into the material was a major concern. Figure 13 indicates that the material was likely to be porous at these pressures as fluid appeared to be leaking through the upper interface of the material. A discussion with the manufacturers of the graphite confirmed this level of porosity and it was suggested that using thermally cured phenolic resin impregnated graphite could solve this problem.

Figures 14 and 15 show the components used in the preliminary test runs.

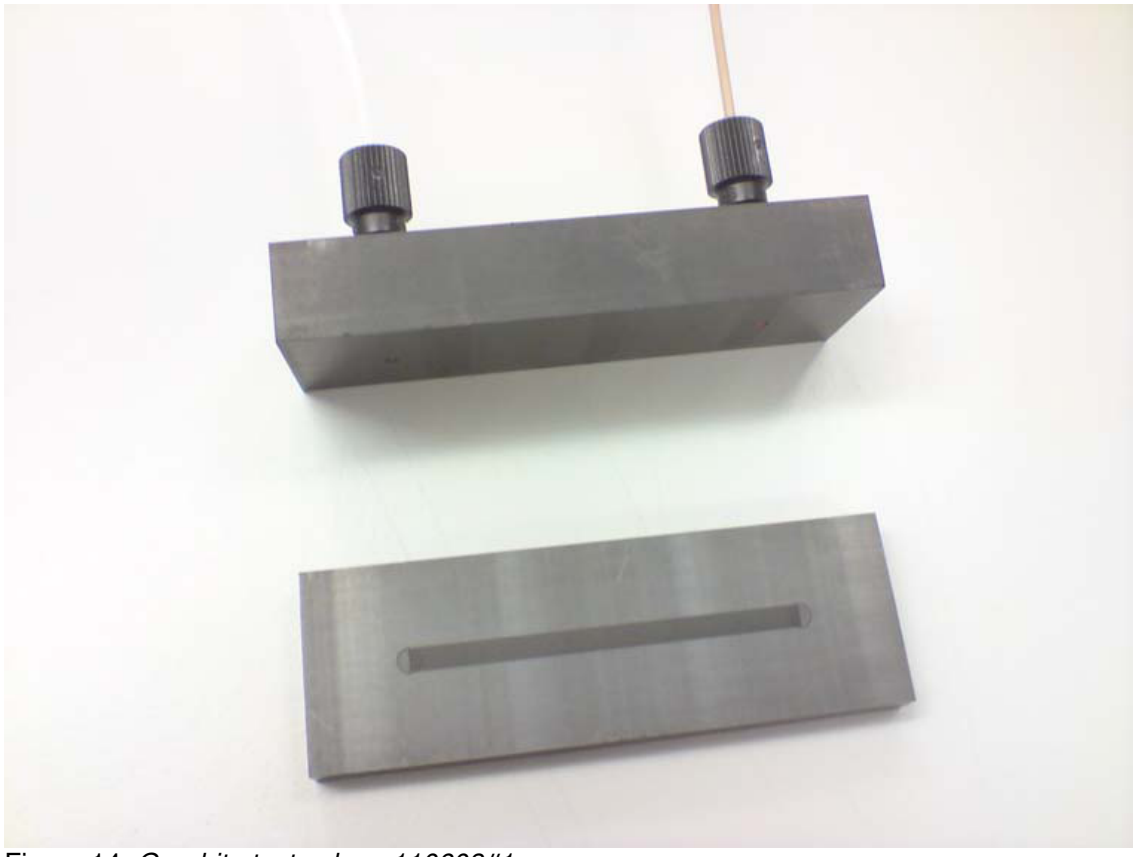

Figure 14*. Graphite test column110608#1*

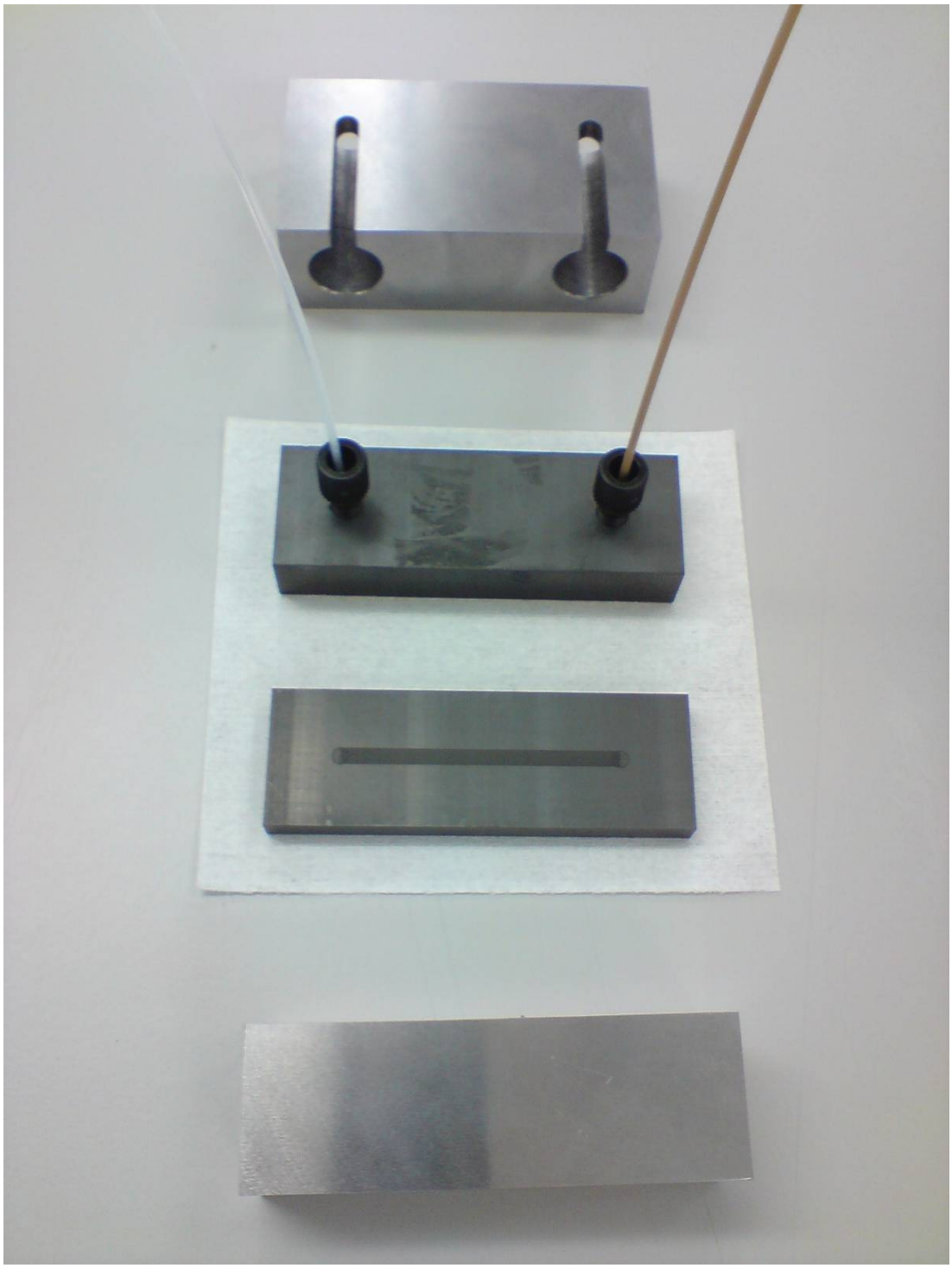

Figure 15*. Graphite test column110608#1 with stainless steel blocks to protect inlet and outlet fluidics.*

1.5 Phase Two

1.5.1 Revised Column Design

A project revision and review detailed the following requirements for the test column:

- A flow distributor was required to distribute the analyte sample at equal concentrations across the column; this is shown in figure 16.
- An on-chip injection point should be incorporated before the flow distributor (shown in figure 16).
- A large array of pillars machined at 45 degrees to the direction of the fluid flow was required.
- Pillars should be laser machined to as large a depth as is reasonably possible, and with the smallest inter-pillar gap.
- A 50mm distance between inlet and outlet centred on the 76mm x 26mm graphite blocks was nominally selected as an initial column design.
- An improvement in the compression seal through polishing methods was desired.
- Integration with the ESI detector on the Surveyor MSQ was desirable.

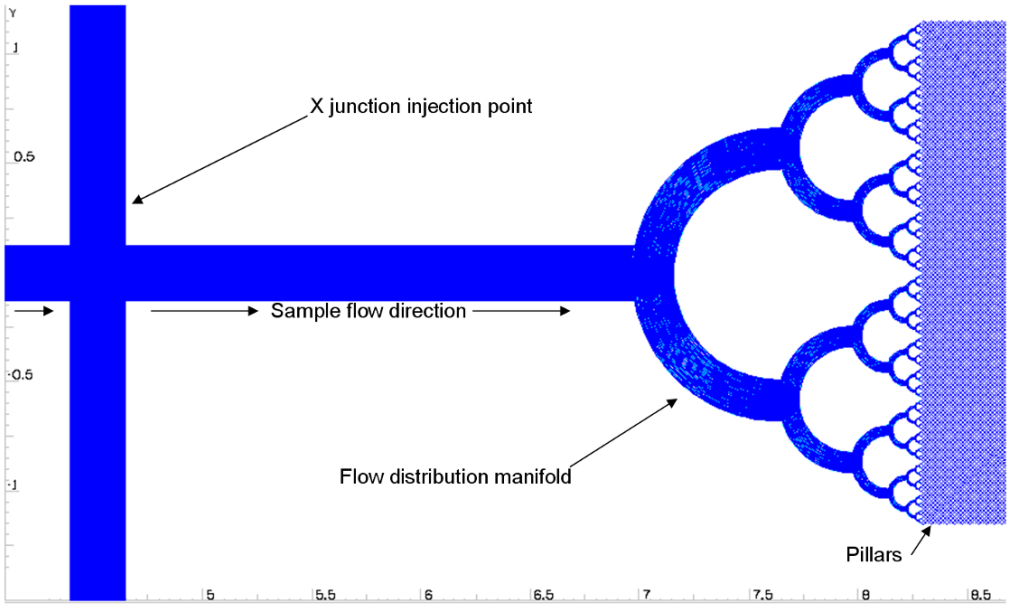

Figure 16. *The inlet side of the CAD file used to create the flow manifold, on-chip injector and pillars.*

1.5.2 Compression Sealing

With the relative success of compression based sealing, the stainless steel and graphite plates were modified to accept screws to bring the compression sealing on board the chip (the component parts are shown in figure 17 and the assembled device shown in figure 18). This was to allow better inspection of the seals and remove the requirement of a large workshop vice, therefore allowing the device to be placed much closer to the detector.

Stainless steel top compression plate with sample injector holes.

Graphite interface plate showing the connection positions for inlet, outlet and injector ports.

Laser machined graphite stationary phase plate with fluidic Interface tracks.

Stainless steel bottom compression plate tapped for M4 screws.

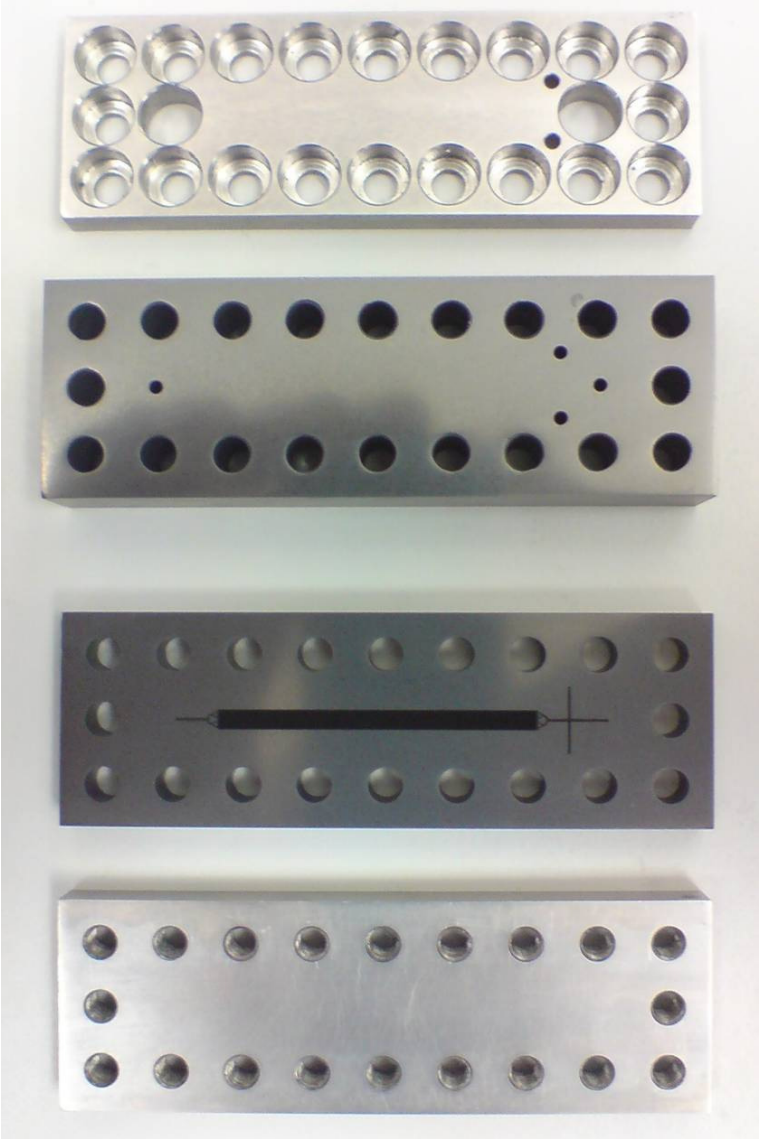

Figure 17.*The components layers of the device before assembly.*

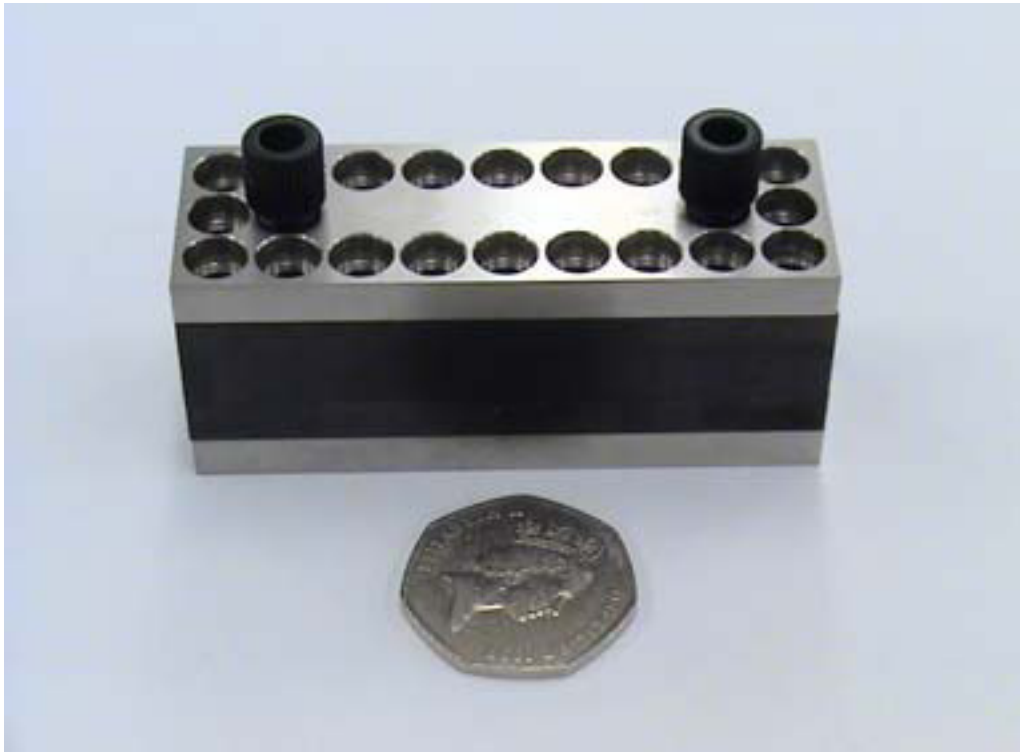

Figure 18. *The assembled device, showing an early version without the integrated sample injector.*

1.5.3 HPLC Interface

1.5.3.1 Detection

It has been previously reported that micropillared chromatography devices have utilized fluorescence imaging or integrated detectors (Fonverne, *et.al*.) However, the integration of these to a conventional HPLC offered limited options due to the flow-cell volume which required higher flow rates than could be supplied through the prototype separations column.

The fluorescence imaging of separations through a fused-silica window was initially trialled but this was quickly abandoned as the 15µm channel depth only provided a very short light path.

UV detection was also considered but was deemed unsuitable due to the flow-cell being too large for such a low flow rate device as the separations column prototyped here.

ESI MS detection: This mass spectrometry method was considered the most viable option for detection. The device could be connected directly to an ESI probe using 0.005" I.D. PEEK tubing. This would require a small slot to be cut into the door of the ESI chamber to allow the tubing to couple directly to the input (figure 34). A make up flow can be used to increase the sample quantity to the minimum level required for the instrument. Such a configuration has been employed elsewhere (Lazar et al.1999).

1.5.3.2 Sample injection

A nano litre (nL) volume x-junction sample injector was laser machined on the chip to deliver an appropriate analyte sample volume for the column capacity. Due to the low volumetric capacity and available surface area of the graphitic device it was deemed inappropriate to use a traditional HPLC auto-sampler injector (typically 5-20 µl sample volume) to introduce the sample into the mobile phase flow, since no temporal resolution would be achievable between retained and non-retained species due to the size of the injection sample slug. It was also reasoned that with the employment of an on-chip sample injector the reduced distance required for the injection slug to travel from the point of injection to the column itself would reduce axial band broadening associated with Poiseuille flow over longer distances, whilst also eliminating band broadening associated with macro/micro interfacing if the injection were to be made off-chip.

1.5.3.3 Test Sample

Analytes

The chemical structure of acrylamide (expected mass to charge ratio m/z = 71.5 – 72.5) is shown in Figure 19 and that of Hydrocortisone (expected m/z = 362.5- 363.5) in Figure 20. These were chosen as test samples as they are expected to behave very differently in the test column. Acrylamide is expected have little interaction with the walls of the graphitic stationary phase and, therefore exhibit a short retention time. Hydrocortisone is expected to have a

much longer retention time due to greater interaction with the walls of the stationary phase.

Acrylamide and Hydrocortisone can both be detected with positive ion mode. This would usefully remove the requirement of the ESI MS detector switching between positive and negative ion detection modes.

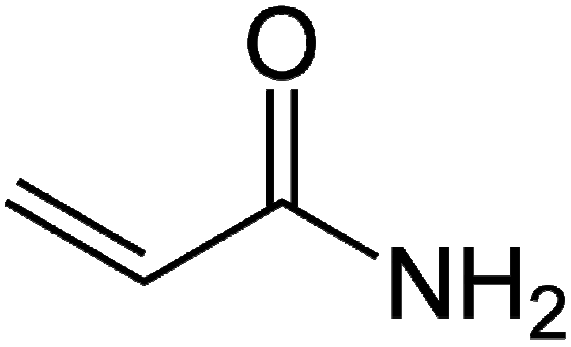

Figure 19. *Acrylamide C_3H_5NO chemical structure*

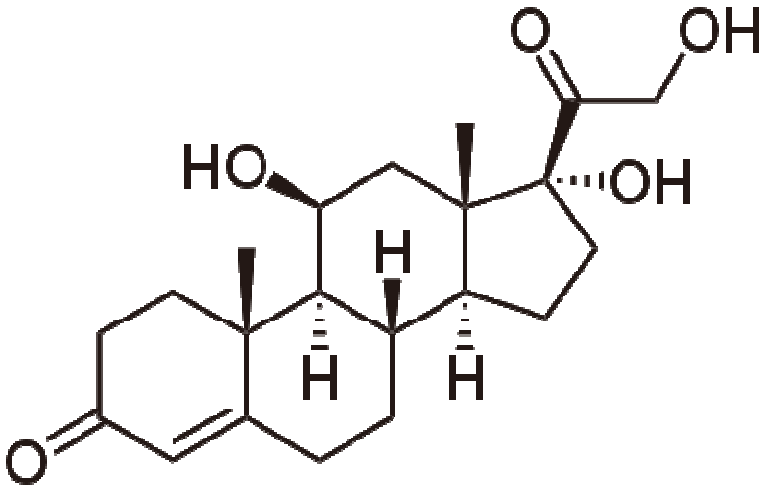

Figure 20. Hydrocortisone $C_{21}H_{30}O_5$ Chemical structure

Mobile Phase

The mobile phase was composed of water and methanol (75%/25% respectively), to which 0.25% acetic acid was added to ensure that the positive polarity was maintained in the electrospray head.

Make up flow

The make up flow was composed of methanol with 1% acetic acid to ensure that the positive polarity was maintained in the electrospray head.

1.5.3.4 Mobile Phase Pumping

Due to the low fluid volume of the laser machined fluid ducts, standard HPLC pumps could not supply the required low flow rate through the device. A Rheos 2000 pump was utilised (Figure 21) to deliver these low flow-rates for the mobile phase without the need for splitting the flow.

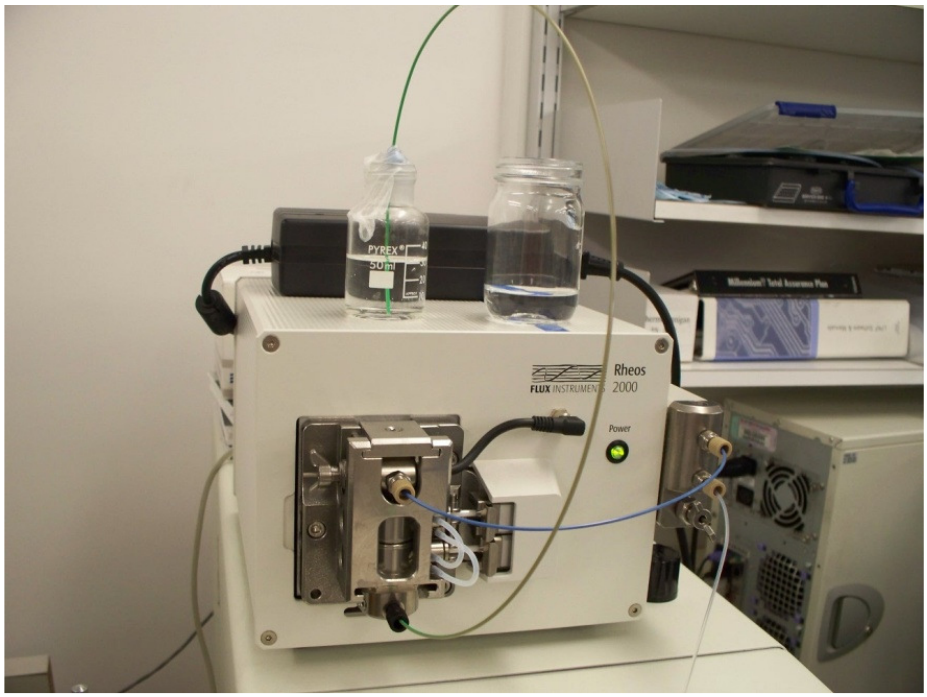

Figure 21. *Rheos 2000 HPLC pump used for mobile phase pumping*

1.5.3.5 Make up pumping

Due to the low flow through the laser machined column, the flow was required to be increased before the detector to satisfy the minimum flow rates of 2µl/minute specified by the manufacturer. A co-axial make up system was used where the outlet of the graphitic separations column entered a narrow fused silica capillary which passed through the central hole of a T-junction union (Figure 22). This fused silica capillary terminates in the centre of a wider bore capillary carrying the make-up flow to the MS detector. The make-up pump used the internal pump integrated within Thermo Fisher Surveyor HPLC.

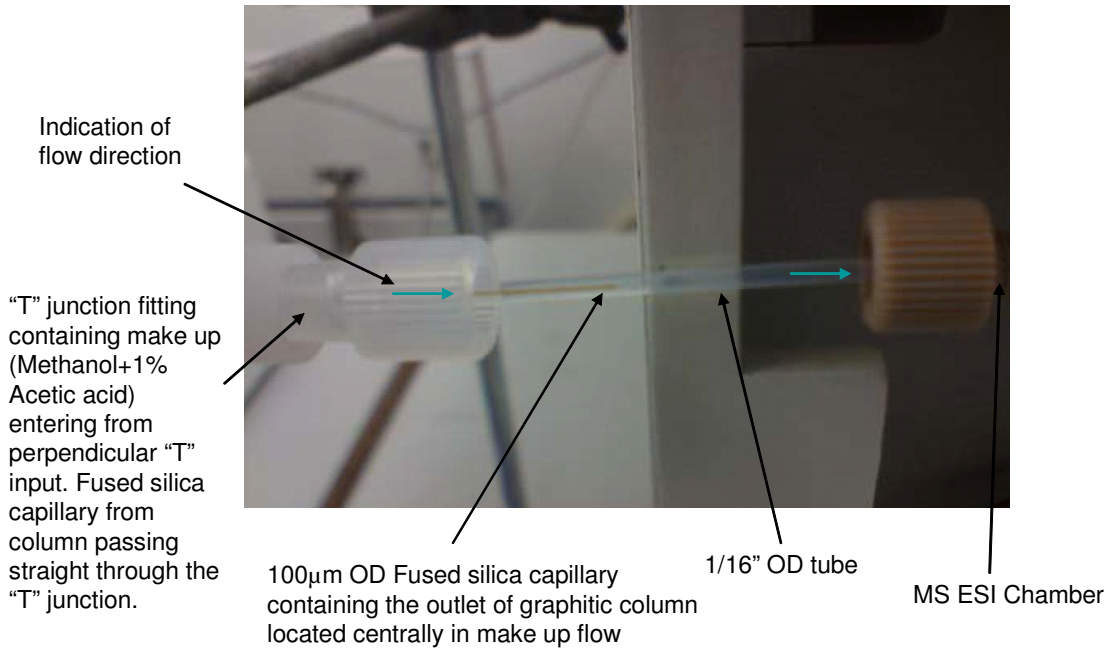

Figure 22. Close-up view of co-axial make-up. The outlet of the graphitic separations column enters a narrow fused silica capillary which passes through the central through hole of a T-junction union, terminating centrally in a wider-bore capillary carrying the make-up flow to the MS detector.

1.5.4 Graphitic material

The original graphite used in Chapter 4 was replaced with graphite impregnated with phenol formaldehyde resin and then thermally cured. This change was instigated by the porosity issues relating to the graphite used in Phase 1 where leakage was detected through the rear of the material (figure 13). The impregnated graphite was expected to be less porous and should have solved the porosity issues. However, it was also considered that the less porous graphite could reduce the column effectiveness by reducing the surface area of the graphite pillars. The column dimensions remained the same and the appearance was similar. The polishing which made use of diamond paste in the earlier tests was improved and the best results were achieved with cerium oxide particles and water. Cerium Oxide is commonly used to polish optical materials such as telescope lenses. A variety of polishing methods were attempted which included polishing pads, 0.25µm diamond paste and polishing disks. The simplest method and the one which gave the best results, used tissue, Cerium Oxide optical polishing powder and water.

1.5.5 Polishing Process

The procedure for polishing graphite was deduced from trial and error, checking the roughness by optical inspection.

Preparation. (Figure 23)

- Lay flat approximately 4 layers of tissue paper on a flat surface, wet the tissue with water and add a small quantity of cerium oxide optical polishing powder.

Polishing Process (Figure 24)

- Place the surface to be polished onto the tissue and move backwards and forwards in the long axis direction for approximately 1 minute or until damage to the tissue occurred. Wash and dry the graphite block, inspecting and repeating on a new area of tissue or new tissue if required. Repeat until desired finish is achieved.

Comparison (figure 25)

- Figure 25 shows the finish attainable after about 6 polishing cycles which take approximately 10 minutes. The level of mirror finish allowed distant objects to be seen as a reflection. The unpolished graphite block shows the starting surface with grinding marks. These were successfully removed during the polishing process. Figure 26 shows the flatness achieved in the polishing cycle.

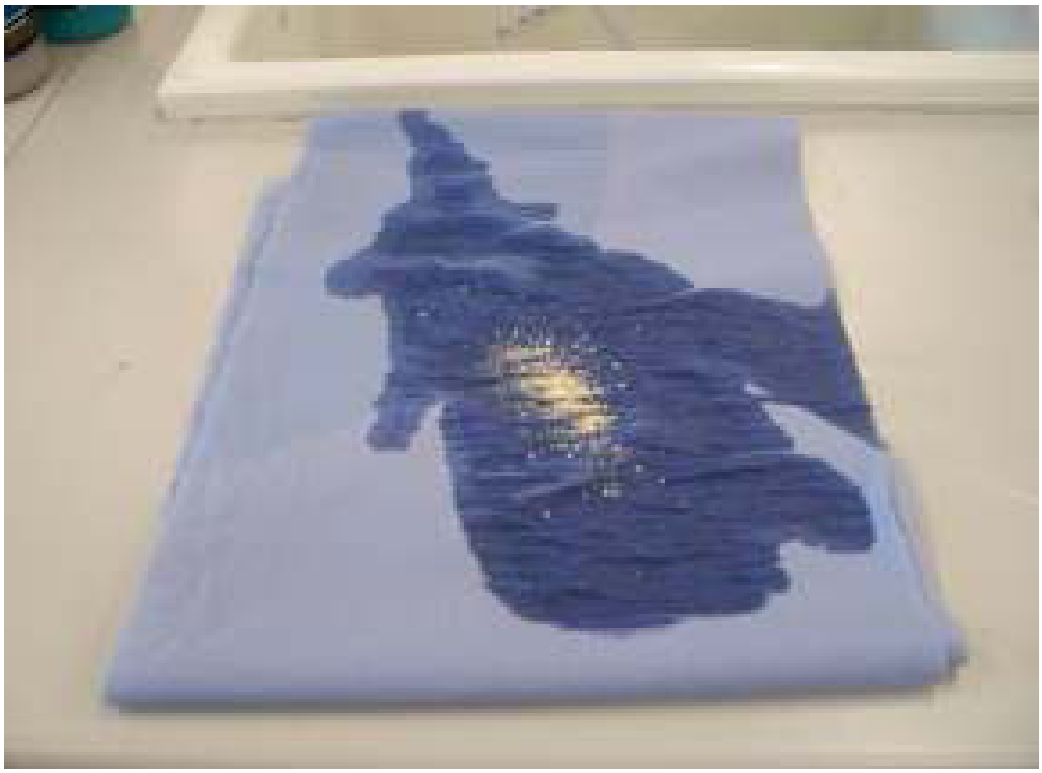

Figure 23. *Polishing method preparation, comprising of flat tissue, water and cerium oxide powder.*

Figure 24. *Polishing process, the arrows indicating the forward and backwards motion in the long-axis polishing direction.*

Figure 25. *A visual comparison between the as supplied, ground finish graphite substrate and the polished graphite substrate.*

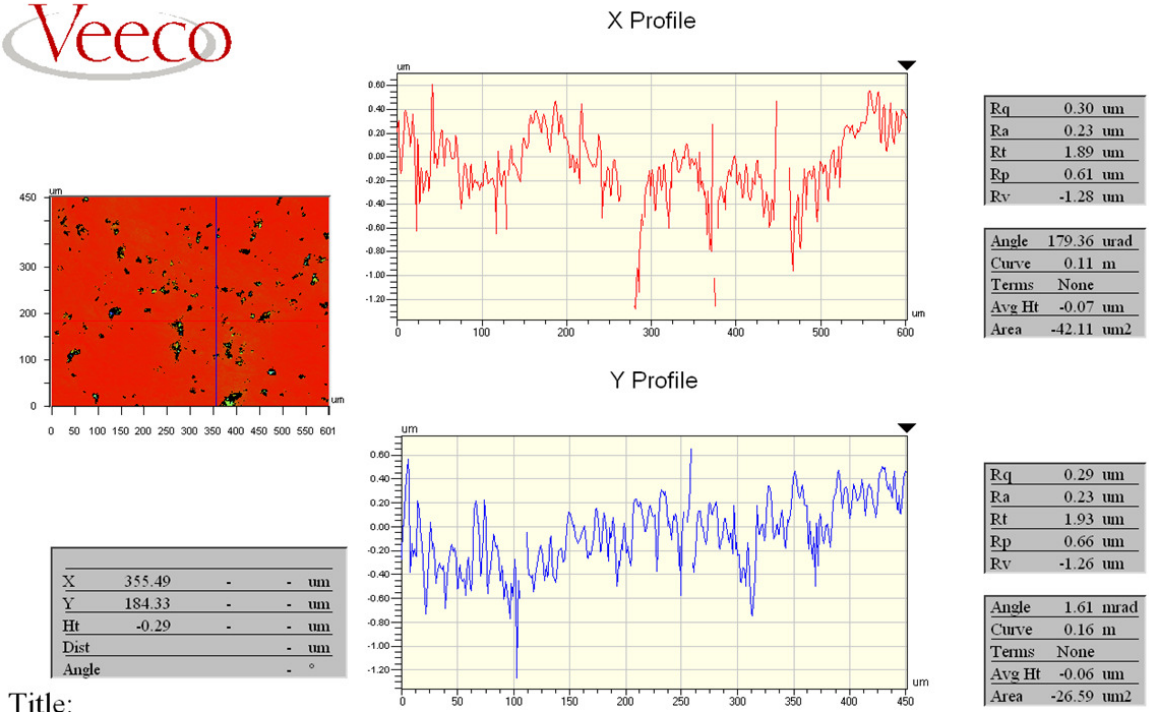

Figure 26. A Veeco surface analysis plot of the polished graphite surface indicating an Ra of 0.23µm.

1.5.6 Laser machining

The Exitech M2000EF workstation was set up for the machining of the graphite surface. A microscope objective was set up with a viewing camera to focus at the same work-piece height as the lens used to focus the femtosecond laser lens and the chuck was levelled using the viewing camera so as to ensure that the laser machining maintained the same focus level across the graphite block.

The power level was set at 0.04W using the polarising beam splitter to attenuate the laser power. This can be controlled remotely in the process software and is rotated in order to set the power. The power meter which is built into the sample chuck gives a direct readout of the power measured at the workpiece.

The graphite block was placed on the chuck polished side upwards and held in position using the chuck vacuum. The rotation stage was rotated to align the input and output ports with the X stage motion. The camera to laser beam offset was set by machining 1. A small spot on an adjacent sample. 2. Measuring the distance from the spot machining position to the centre of the camera when displayed on the camera monitor with overlaid alignment marks. This ensured a high positioning accuracy with the pattern on the sample.

A jet of air at a flow rate of 5l/minute was directed to blow under the lens. This minimized debris build up on the lens which could otherwise attenuate the beam. This would have affected the machining depth across the sample.

The CAD file was set up to give the start (0,0) point at the outside end of the inlet port. This point was aligned under the viewing camera and the chuck was moved by the laser offset so as to position the beam in that position. The CAD file was designed to run into the inlet and outlet ports by 50µm to ensure that a fluid path existed even if a minor misalignment occurred.

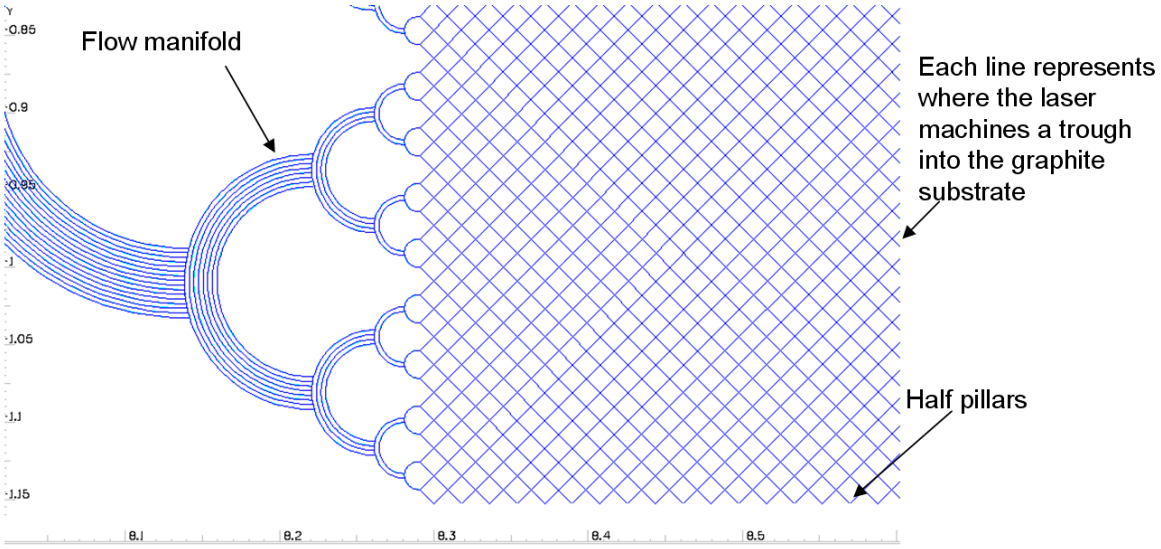

Figure 27. A *close up of the CAD at one end of the column. Note the half pillars on the edges machined in an attempt to reduce band broadening when in use. Each line represents where the laser will remove graphite from the prototype separations device. The axis scale is in mm.*

As shown in figure 27 the G code program, created using Alphacam from the CAD file, was then run and the machine commenced the subtractive machining process which ran for approximately 18 hours. The laser was allowed to run initially for several hours to reach thermal stability. The power was then set at 0.04W and the process of machining commenced. The machine was left running without operator assistance for the full duration. The finished machined column showed no obvious structure variation of the type associated with power variation over time. The machined pillars are shown in figure 38 and the full device design (CAD) is shown in figure 29.

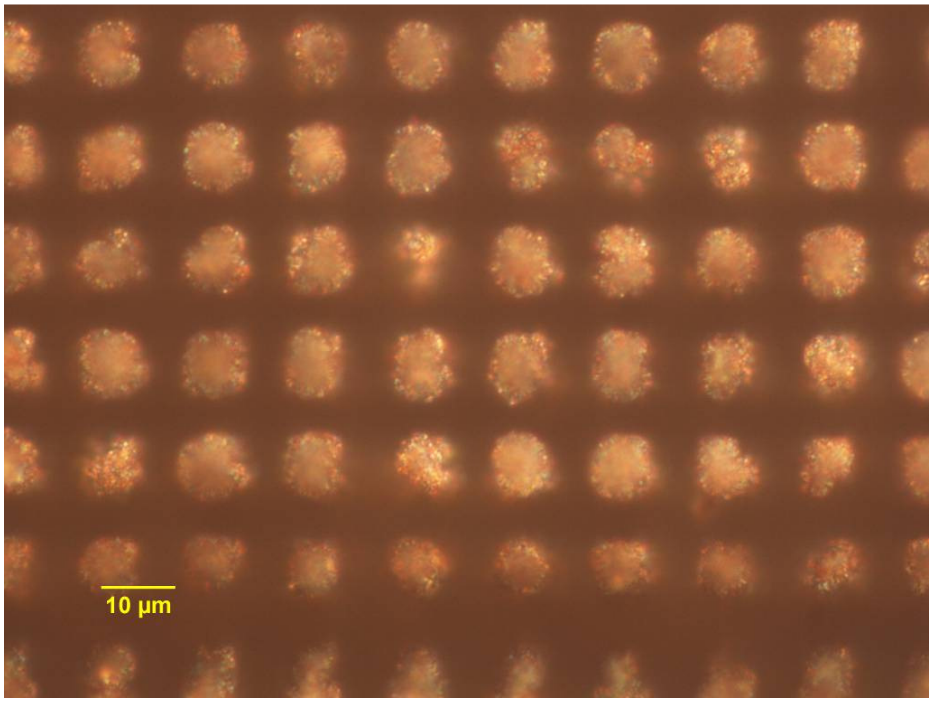

Figure 28. *Optical microscope picture of prototype graphitic column array: 14µm inter-pillar pitch, 6µm streets machined with the Femtosecond laser at 0.04W.*

Figure 29. *The complete CAD file used to write the separations column clearly showing the position of the X junction to the left. The CAD was written in Alphacam and AutoCAD and comprised of over 3200 component parts once translated into G-Code.*

1.5.7 Experimental Set up

The following pictures and diagrams (Figures 30 – 36) show the integration of the graphitic separations column with the Mass Spectrometer including the attempted use of a rheodyne valve for the sample injection switching. The latter proved unsuccessful due to the void volume, internal to the switch, being greater than the volume of the prototype separations column. A more primitive method was developed involving the timely opening and closing of valves and physical compression of the syringe pump to introduce a plug of analyte across the X junction. The X junction analyte injection pipes are clearly shown on figure 30 and figure 35.

Figure 30. *Assembled graphitic device interfaced with flow-make up to provide a sufficient volumetric flow for electrospray ionisation and mass spec analysis.*

The equipment layout is shown in figure 36.

Figure 31. *Rheodyne flow switching configuration proposed for sample injection and elution.*

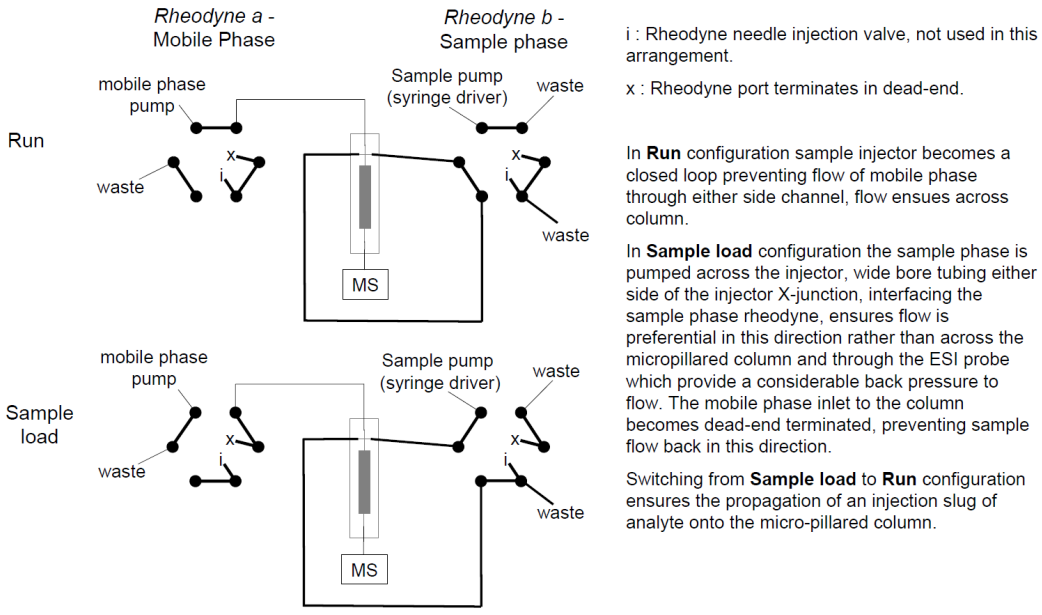

Figure 32. A schematic of the *rheodyne flow switching configuration proposed for sample injection and elution. Unfortunately the void volume introduced on rheodyne switching resulted in failure to deliver sample phase into the mobile phase flow stream. Consequently a manual injection method was developed (Figure 34).*

Figure 33. *A close up of the cut-out machined into the Surveyor MSQ door to allow the tubing to directly interface to the ESI input.*

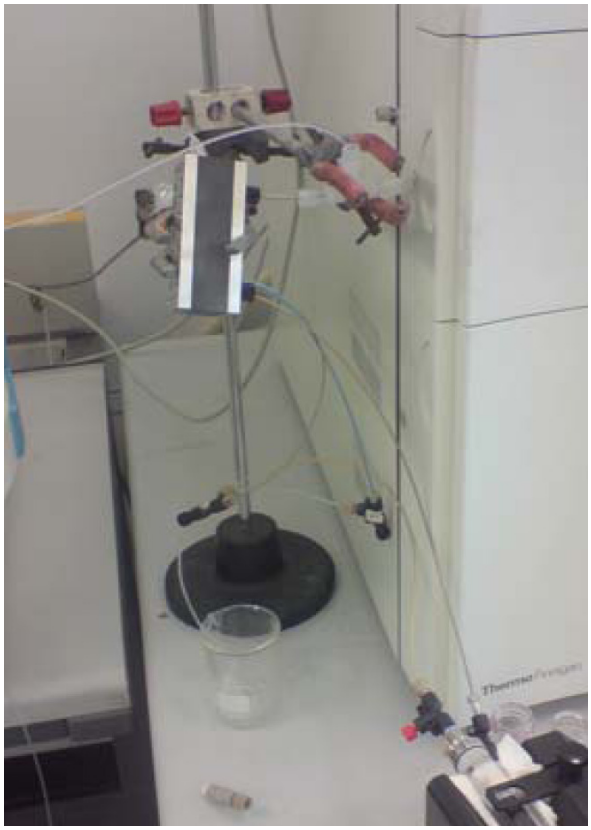

Figure 34. *Manual valve-controlled sample-injection setup to introduce sample phase from the pictured syringe into the mobile phase flow stream, on-chip, utilising the X-junction sample injector.*

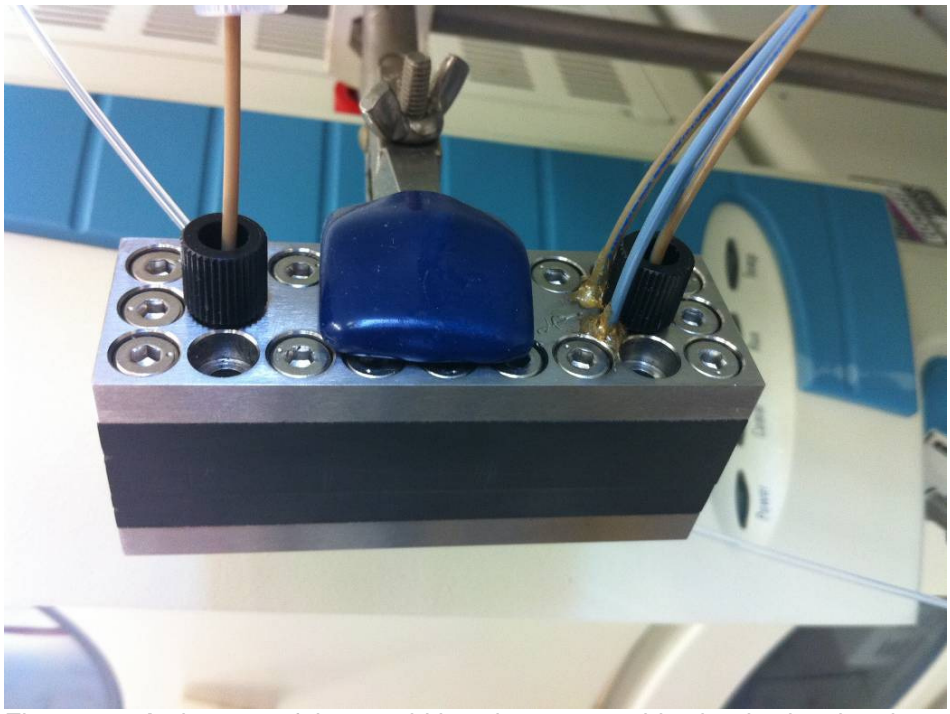

Figure 35*. A close up of the graphitic column assembly clearly showing the sample X junction injector connections.*

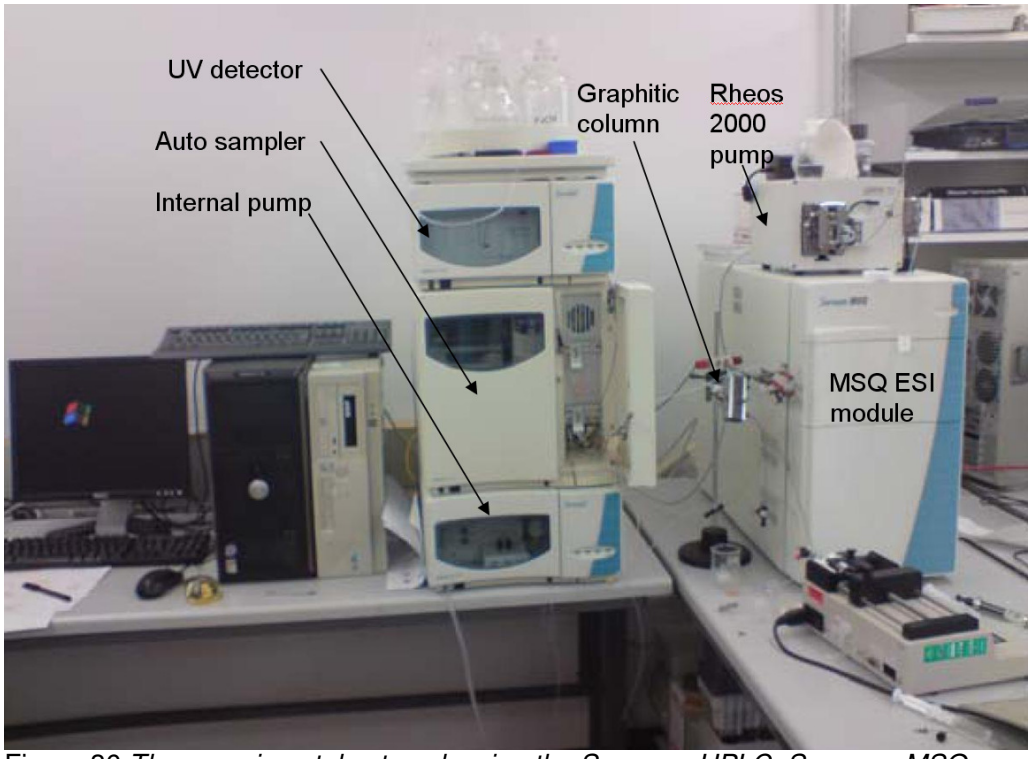

Figure 36.*The experimental setup showing the Surveyor HPLC, Surveyor MSQ, Graphitic column, Rheos 2000 pump for mobile phase delivery, KD scientific syringe driver for sample phase delivery. A computer running Xcalibur™ MS acquisition software and a computer running Janeiro II 2.6 the Rheos pump control software were employed.*

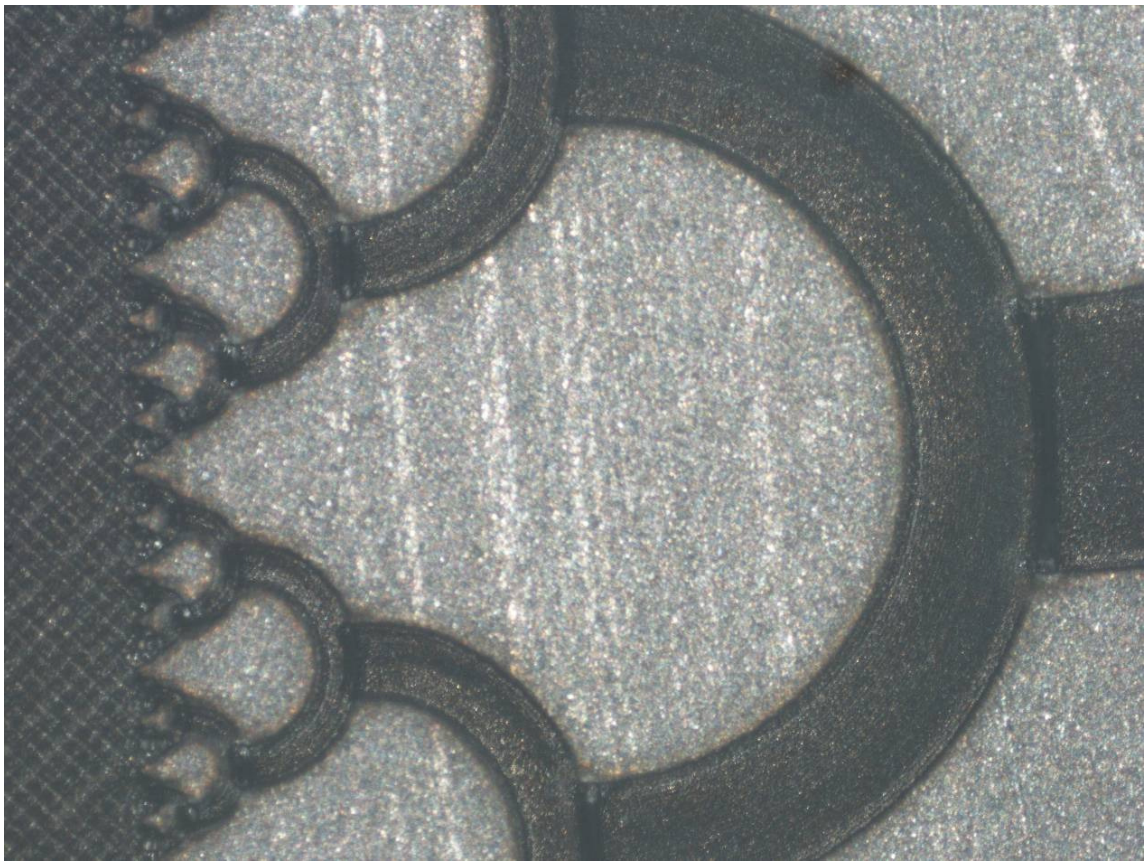

Figure 37. *An optical microscope picture of a section of the laser machined flow distributor and column array.*

1.6 Results

The laser machining and fluidic sealing of the device worked successfully in order to advance to the testing stage. A section of the laser machined flow distributor and array is shown in figure 37.

Several difficulties were encountered in the operation and testing of the graphitic separations device. However, an adequate system was devised for preliminary evaluation of the device performance, as described below.

At the desired operational flow rates required (0.001 ml/min) traditional HPLC pumping options were not applicable. Therefore, a low-flow-rate capable Rheos 2000 pump was utilised for ultra-low-flow rate mobile phase delivery. However, flow at the desired rate proved unstable, and thus a pumping strategy utilising residual pumping pressure after pumping at higher flow rates was utilised.

The Rheos 2000 pump was externally operated by a PC running Janeiro II 2.6 software. When pumping a mobile phase (75% H_20 / 25% MeOH + 0.25% acetic acid) through the separations device at programmed flow rates of 0.001 ml/min, a back-pressure of approximately 35 psi was typically recorded on the PC. However, transit times of non-retaining species across the device were found to be sporadic and the pumping unreliable. At higher flow-rates the back pressure monitor was observed to fluctuate in a cyclic manor, the consequence of which was pulsatile flow of mobile phase through the separations column. This was undesirable for the successful evaluation of the device. As a result, prior to each injection, the flow-rate of the mobile phase was increased to 0.005-0.02 ml/min for several minutes, before reducing the pumping flow rate to 0.001 ml/min. The residual back pressure on the pump was closely monitored as it steadily fell from around 200-500 psi to approximately 35 psi. This process not only purged the column between sample runs, but enabled manual sample injection at desired back pressures providing stable, non-pulsatile mobile phase flow through the device. Manual injections were made typically at recorded back pressures of between 80 and 200 psi.

Sample injections were made by running a solution of acrylamide and hydrocortisone across the x-junction sample injector. Initially, this was attempted using a rheodyne flow switching setup but this proved unsuccessful. It was proposed that this was due to the negative pressure induced on switching of the rheodyne valve which replaced the sample in the injector x-junction with mobile phase. A second approach utilised in-line on/off valves either side of the injector x-junction, on the PEEK tubing inlet and outlet capillaries. It was reasoned that mobile phase could be pumped constantly and the sample phase introduced by switching the valves as follows:-

1) The valve on the injector outlet was opened, diverting mobile phase flow out through this exit due to the lower resistance to flow by this route than through the pillared column.

2) With a syringe driver turned on to deliver the acrylamide and hydrocortisone test mix to the device (flow rate 0.01 ml/min), the valve on the injector inlet was opened, allowing delivery of the sample phase across the injector x-junction.

3) The valves on the injector inlet and outlet were closed simultaneously, stopping the flow of sample phase to the device and forcing the flow of mobile phase through the pillared graphitic column. This took the slug of residual sample phase lying in the injector x-junction with it for subsequent separation on the column.

However, in practice, this method of sample injection proved unsuitable due to the rapid loss of pressure of mobile phase upon opening of the valve on the injector outlet, resulting in a failure of flow resumption through the column on the closing of the valves due to an insufficient back-pressure to support mobile phase flow. The resumption of locomotive flow through the device proved to be sporadic and unpredictable.

Ultimately, a somewhat less accurate, although reproducible, method of sample injection was developed which involved the rapid addition of a small volume of sample phase flow (added via the sample injector inlet), to the continuously flowing mobile phase flowing through the pillared column. (i.e. the valve on the injector outlet remained closed at all times, with the valve on

the injector inlet opened very briefly (1-3 seconds) to allow a small addition of the analyte sample). Injection by this method proved problematic since the pressure requirement for the flow of the sample phase onto the device had to be greater than the back pressure supplied by the mobile phase pump delivering mobile phase through the graphitic pillared column, or else the mobile phase flow would simply divert into the sample injector inlet. This requirement made the delivery of the sample test mix using a syringe driver impossible since it was unable to provide sufficient pressure. Consequently the injection had to be performed manually by physical compression of the syringe driver manifold at the time of opening the sample phase inlet valve. As such, the quantity of sample injected was unknown; although the measured response at the MS detector was found to be reproducible on repeat injections and the injection size could be modulated by varying the time the inlet valve remained open (Figure 38). As such, it was apparent that the volume of sample phase being injected was potentially greater than the injector x-junction intersection volume, suggesting that the sample phase was flowing up/down the mobile phase flow stream during the injection. This resulted in a greater sized sample slug than desired, reducing temporal resolution of the analyte separation. Despite this undesirable feature of the evaluation method, the results achieved were strongly encouraging, since it is anticipated that an improvement of the sample injection system, which would be readily achievable with a second low-flow-rate pump, would dramatically improve temporal resolution of the eluting analyte peaks. Figure 39 shows the full detected signals for both acrylamide and hydrocortisone clearly showing the differential retention of acrylamide and hydrocortisone on consecutive injections of a combined mixture of the two analytes with ESI mass spectra viewed at each of the specific mass ranges for acrylamide (71.5-72.5 m/z) and hydrocortisone (362.5-363.5 m/z). Figure 40 shows time elapsed screen shots of the Surveyor MSQ showing the acrylamide and hydrocortisone peaks occurring at different times.

Mobile phase	Mobile phase delivery pressure	Test sample	MS flow make-up	Probe temp (ºC)	Needle (kV)	Mass ranges	Scan time	Cone voltage
H_2O/MeOH (75/25) + 0.25% acetic acid	varied between 80-200psi to alter mobile phase flow rate	Acrylamide (0.1 mg ml^{-1}) and Hydrocortisone (0.1 mg ml^{-1}) in H_2O/MeOH (75/25) + 1% acetic acid	0.2 ml min^{-1} MeOH + 1% acetic acid (0.2 ml min^{-1})	519	5.0	72 +/- 2 (gain 150) 363 +/- 2 (gain 50)	0.08s	55

Table 1. *The set up parameters and conditions for testing of the prototype laser machined graphitic separations column.*

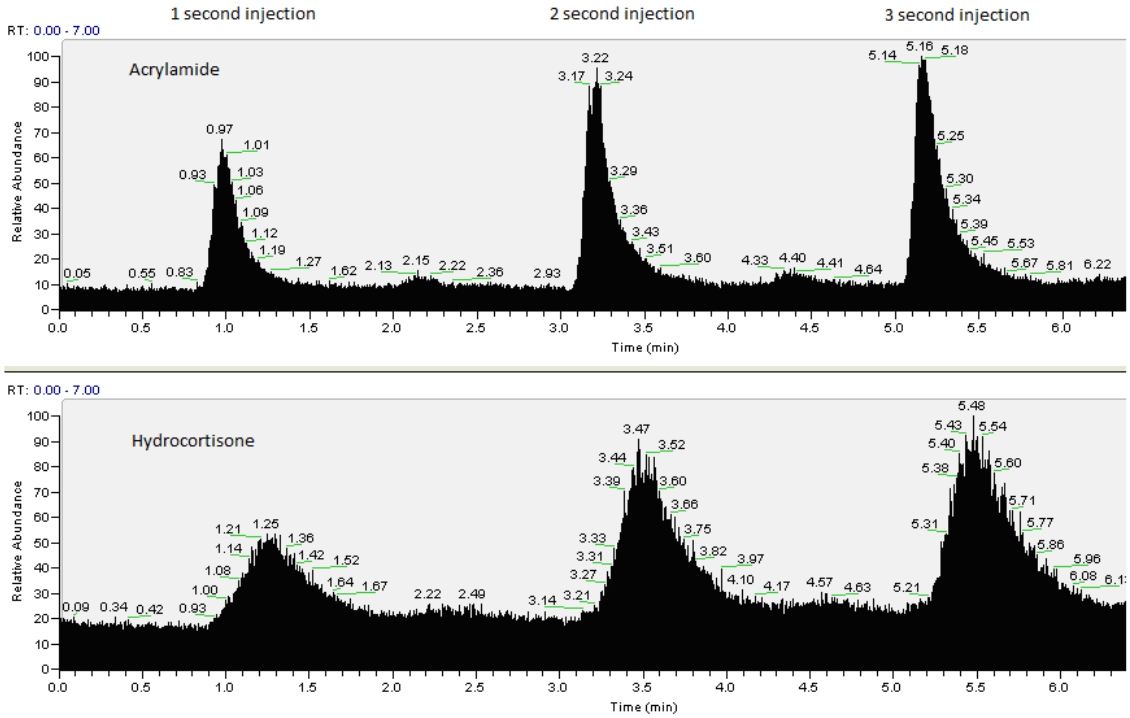

Figure 38. *3 repeat injections of the acrylamide/hydrocortisone test mix. In each successive injection the injector valve was opened for a decreased duration (~3, ~2, ~1 seconds respectively), demonstrating the flooding of the sample injector x-junction. This results in a larger than desired sample injection volume and therefore loss of temporal resolution in the separation as the injection slug volume becomes increasingly significant compared to the low volume of the separations column itself. It is proposed that a dramatically improved separation may be achieved on development and integration of a finely controlled, on-chip, sample phase injector.*

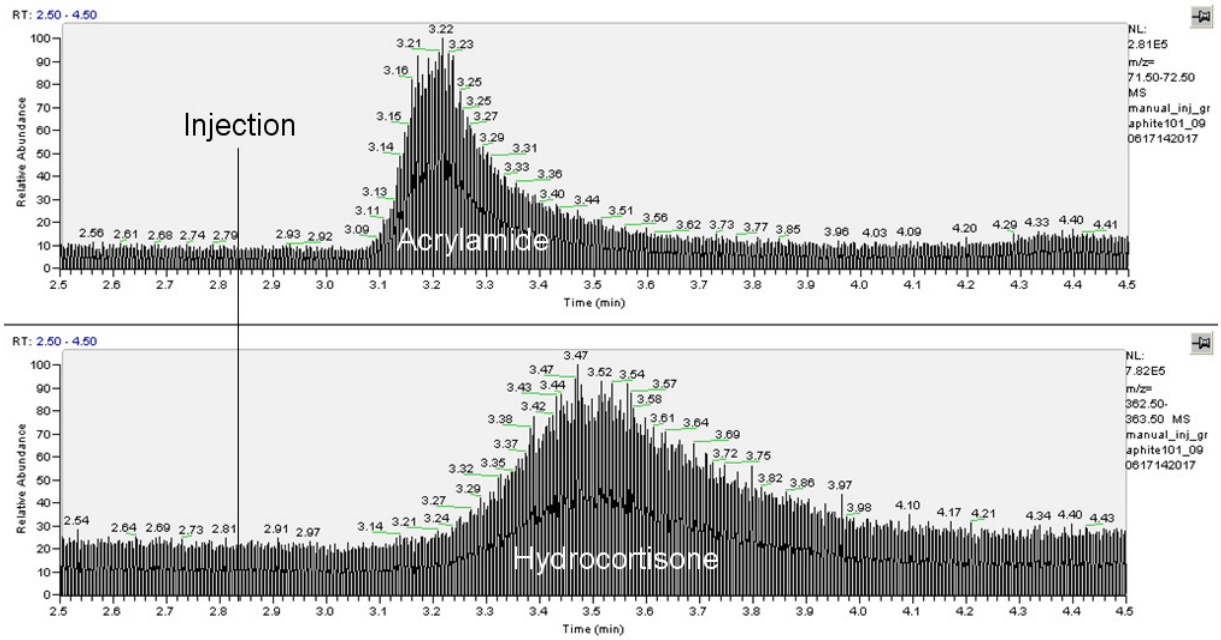

Figure 39. *The differential retention of acrylamide and hydrocortisone on consecutive injections of a combined mixture of the two analytes. ESI mass spectra viewed at each of the specific mass ranges for acrylamide (71.5-72.5 m/z) and hydrocortisone (362.5-363.5 m/z).*

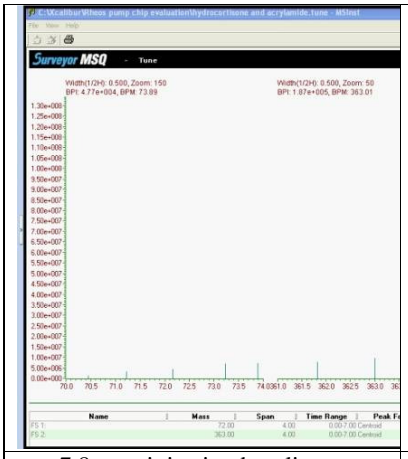	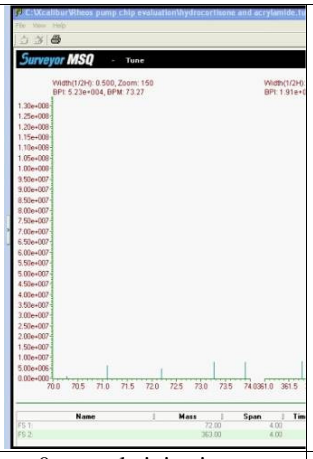	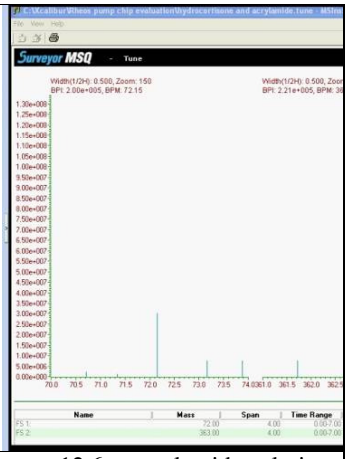
t = -7.8s pre-injection baseline	t = 0s sample injection	t = 12.6s acrylamide elution begins
	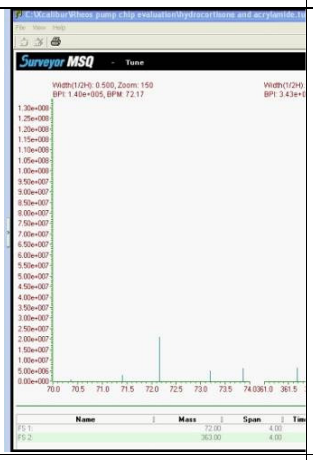	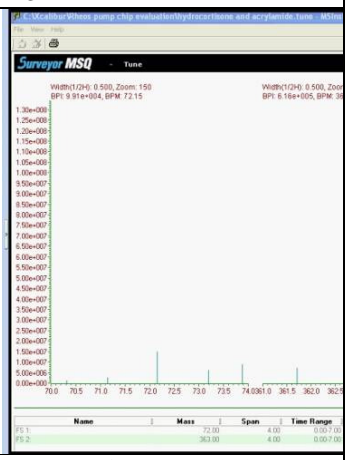
t = 14.4s acrylamide peak	t = 22.2s tail of acrylamide elution, hydrocortisone elution begins	t = 25.8s co-elution of acrylamide and hydrocortisone
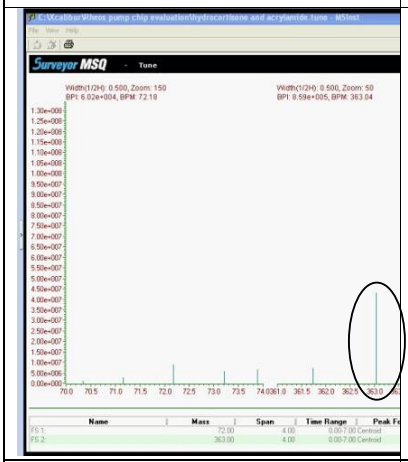	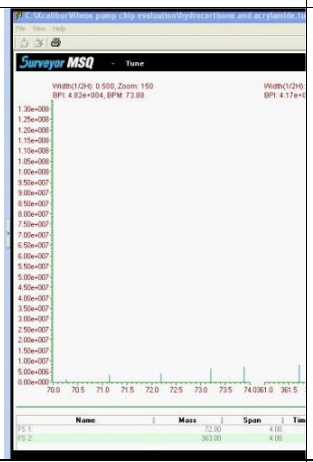	
t = 34.2s hydrocortisone peak	t = 52.2s hydrocortisone tail	t = 73.8s return to baseline

Figure 40. *Time elapsed screen shots of the Surveyor MSQ showing the Acrylamide and hydrocortisone peaks occurring at different times.*

1.7 Discussion and Conclusions

The differential retention of two analytes in a single sample phase has been successfully demonstrated using a laser micro-machined graphitic microfluidic device interfaced to a macro-scale mass spectrometer and traditional HPLC-style equipment. The miniaturised separations platform shows considerable promise for future development of high efficiency, rapid chemical separations. The microfluidic device format enables run times of less than 1 minute with low reagent consumption and low requirement for analyte matrix volume, with highly ordered pillared stationary-phase structure and flow distribution architectures improving theoretical separation efficiency over traditional microsphere packed-bed columns. Ultimately, a solid-state microfluidic graphitic separations device may be used at high temperatures and pressures to enable the use of subcritical water chromatographic techniques, offering practical, safety and environmental advantages over traditional organic solvent orientated separation methodologies. Towards this aim, the reported device has been demonstrated to withstand high pressure flow without leakage (~350 psi), which may be further improved through the use of a polyamide imide bonding resin between substrate layers.

Opportunities and Challenges

Although a significant difference in retention of the two eluting test species was demonstrated, 100% resolution of the component peaks was not achieved under the evaluated test conditions. This was reasoned to be due to several contributing factors which may be significantly improved upon with further development of the device and evaluation conditions as discussed below.

Improved pumping options

Ultra-low-flow rate, precision controlled, mobile phase delivery is crucial. The Rheos 2000 pump, although an improvement on traditional HPLC pumps, proved too unstable to consistently deliver a prescribed flow rate and a

residual pressure delivery method had to be employed following pumping at higher flow rates. A head-space pressure regulated delivery method for mobile phase delivery would enable precise, low-flow rate control. A comparable pumping solution would also be desirable for sample injection.

Improved sample injection process

Due to the failure of the originally implemented rheodyne flow switching injection method, and subsequent failure of the available syringe pumps for sample phase delivery to the chip at the required operational pressures, the manual sample injection process provides significant scope for process enhancement. The manual method of sample delivery was found to result in flooding of the x-junction sample injector (as evidenced by the increased detection signal with increased injection valve open time) (Figure 39). This uncertainty in injection slug volume may have caused the most significant contribution to peak broadening and failure to completely separate the two compounds, with the injection slug volume approaching that of the pillared separations column itself, significantly reducing temporal resolution of sample injection. It is envisaged that improvement in the on-chip sample delivery process would facilitate enhanced separation efficiency. It is proposed that this process may be improved by the employment of a combination of;

(i) ultra-low-volume rheodyne switching configuration (if available)

(ii) On-chip valve-based flow switching, reliable sample phase flow delivery (i.e. comparable pumping options to those required for mobile phase delivery)

(iii) Implementation of an electro-kinetically driven sample injection methodology.

Parallel fluidic exit and elimination of void volumes

In this prototype device fluidic exits from the graphitic device were orientated perpendicular to the separations column. The right angled turn and void volume introduced at the interface with the PEEK capillary certainly contributed to band broadening on analyte elution from the device. It is proposed that improved performance could be achieved through the embedding of a fluidic exit parallel to the separations geometry. This would

most preferably be in the form of the narrow O.D. fused silica capillary utilised to deliver the chip eluent directly into the ESI-flow-makeup. The reduction in void volume, elimination of the requirement for fluid-reorientation and elimination of the PEEK-fused silica union in the current construction of the ESI-flow-make-up would improve peak resolution. In addition, a reduction in the post-separation flow distance to detector would also be beneficial.

Column transit time

Due to the extremely low volume of the separations column itself, the post-separation eluent flow to the MS detector represents a significant portion of the analysis time, during which band broadening occurs. It can be seen that acrylamide detection begins just 12 s after sample injection (Fig 40). With consideration of the fluidic volume of the post-column flow distributor, graphitic channels, PEEK tubing and fused silica tubing leading to the make-up flow, the transit time across the pillared separation column itself is likely to be less that 5 s. Perhaps this is insufficient for complete separation of the two analyte species. Due to the pumping options available it was not possible to reliably pump at a sufficiently reduced flow-rate to afford greater resolution of separation. It is envisaged that implementation of suitable pumping mechanisms outlined above would significantly enhance performance.

On-chip detection or Integration of ESI probe into device

Integration of a detector on-chip immediately after the separations column would improve resolution of the separation. Possible candidate detection methodologies include incorporation of a UV waveguide or integrated electrical detection. It may also be desirable to integrate an electrospray tip directly into the device to interface the chip eluent more closely with the mass spectrometer. However, this may require adaptation of the Surveyor MS to incorporate the separations chip within the aerosolisation chamber.

Laser machining improvements

Device design enhancements may also be made through improvement of the laser micromachining process. A narrower inter-pillar gap may be achieved

and a wider, longer separations bed of greater pillar density may be produced. However, the requirement for machining time would also increase with the implementation of such a geometry using direct-write laser machining processes. Development of a synchronised mask-projection UV Excimer laser machining method would be anticipated to reduce device production time and also provide the additional advantage of providing the ability to machine higher-aspect-ratio pillars with near-vertical side walls. Further investigations could include >100kHz or MHz pulsed femto or pico-second lasers with high precision scanners to increase write time significantly.

Increasing available graphitic surface area

It may be possible to increase the column capacity through a direct increase in available graphitic surface area within the pillared device. This could be achieved through the introduction of a more porous layer of graphite in the column area or by the growth of carbon within the laser machined column itself.

The post laser treatment of a laser machined column using a thermal laser source in the IR could locally introduce porosity. The success of this may be dependent on the choice of impregnated material.

Final Conclusions:

Several improvements are mentioned above with respect to pump control at low flow rate. However when one considers the relatively huge surface area of conventional porous graphite particles one does consider that a dramatic increase in surface area is the key advance needed here to achieve a step change in differential retention of analytes. Nevertheless, the aim of this study was to investigate whether a laser machined graphitic micro-fluidic device could be manufactured and this was demonstrated for the first time. Testing the microfluidic device at the pressures associated with HPLC was successfully demonstrated, and furthermore, the separation of two (albeit significantly different) molecules in solution was demonstrated, although not with total peak separation.

1.8 Acknowledgements

This work was undertaken at the UK metaFAB nanocentre facility with support from the UK government Technology Strategy Board, Thermo Fisher UK Ltd. and Nikon (UK) Limited.

Bibliography

Broeckhoven,K. Desmet,G.. (2007). Approximate transient and long time limit solutions for the band broadening induced by the thin sidewall-layer in liquid chromatography columns. *Journal of Chromatography A*. 1172 (1), 25-39

Colin,H .Guiochon,G. (1977). Introduction to reversed-phase high-performance liquid chromatography. *Journal of Chromatography A,* . 141 (3), 289-312.

Cunningham,N.Lefevre,M.Dodelet,J.Thomas,Y.Pelletier,S. (2005). Structural and mechanical characterization of as-compacted powder mixtures of graphite and phenolic resin. *Carbon*. 43 (15), 3054-3066.*]*

De Smet,J. Gzil,P. Vervoort,N. Verelst,H. Baron,G, V. Desmet,G. . (2004). Influence of the Pillar Shape on the Band Broadening and the Separation Impedance of Perfectly Ordered 2-D Porous Chromatographic Media. *Analytical Chemistry*. 76 (13), 3716-3726.

Eijkel,J. (2007). Chip-based HPLC: the quest for the perfect column. *Lab on a Chip*. 7 (1), 815-817.

Fonverne,A. Ricoul,C. Demesmay,C. Delattre,C. Fournier,A. Dijon,J.Vinet,F. (2008). In situ synthesized carbon nanotubes as a new nanostructured stationary phase for microfabricated liquid chromatographic column. *Sensors and Actuators B: Chemical*. 129 (2),510-517.

Gilbert, M.T,Knox,J.H,Kaur,B. (1982). Porous glassy carbon, a new columns packing material for gas chromatography and high-performance liquid chromatography. *Chromatographia*. 16 (1), p138-146.

He,B. Regnier,F. (1998). Microfabricated liquid chromatography columns based on collocated monolith support structures. *Journal of Pharmaceutical and Biomedical Analysis*. 17 (6-7), 925-932.

Hemmersbach, P. (2008). History of mass spectrometry at the Olympic Games. *Journal of Mass Spectrometry*. 43 (7), 839-853.

Knox,J. Kaur,B. Millward,G.R. (1986). Structure and performance of porous graphitic carbon in liquid chromatography. *Journal of Chromatography A*. 352 (1), 3-25.

Labat,L. Dumestre-Toulet,V. Goulle,J,P. Lhermitte,M.. (2004). A fatal case of mercuric cyanide poisoning. *Forensic science international*. 143 (2), 215-217.

Lazar,I.M. Ramsey.R.S. Sundberg,S. Ramsey,J.M. (1999). Subattomole-Sensitivity Microchip Nanoelectrospray Source with Time-of-Flight Mass Spectrometry Detection. *Analytical Chemistry*. 71 (17), 3627-3631.

Liu,X.Du,D.Mourou,G.. (1997). Laser ablation and micromachining with ultrashort laser pulses. *IEEE Journal of Quantum Electronics*. 13 (10), 1706-1716.

McClay,J.A. Mcintyre,A.S.L.. (1999). 157NM OPTICAL LITHOGRAPHY : THE ACCOMPLISHMENTS AND THE CHALLENGES. *Solid State Technology*. 42 (6), 1-7.

Ostendorf,A. Bauer,T. Korte,F.Howorth,J.R. Momma,C. Rizvi,N.H. Saviot,F. Salin,F.. (2002). Development of an industrial femtosecond laser micromachining system . *The International Society for Optical Engineering*. 4633 (1), 128.

Park,W.J. Kim,J.H. Cho.S.M. Yoon,S.G. Suh,S.J. Yoon,D.H.. (2003). High aspect ratio via etching conditions for deep trench of silicon. *Surface and Coatings Technology* . 171 (1-3), 290-295.

Pereira,L. (2008). Porous Graphitic Carbon as a Stationary Phase in HPLC: Theory and Applications. *Journal of Liquid Chromatography*. 31 (11), 1687-1731.

Ross, P. Knox, J. H.. (1997). Carbon-Based Packing Materials for Liquid Chromatography: Applications. *Advances in Chromatography*. 37 (1), 121-162.

Shah,L. Tawney,J. Richardson,M. Richardson,K. (2001). Femtosecond laser deep hole drilling of silicate glasses in air. *Applied Surface Science*. 183 (3-4), 151-164.

Sokolowski-Tinten, K. Kudryashov, S. Temnov, V. Bialkowski, J. von der Linde, D. Cavalleri, A. Jeschke, H. O. Garcia, M. E. Bennemann, K. H. . (2000). Femtosecond Laser-Induced Ablation of Graphite. *SPRINGER SERIES IN CHEMICAL PHYSICS*. 66 (1), 425-427.

West,C. Elfakir,C. Lafosse, M. (2010). Porous graphitic carbon: a versatile stationary phase for liquid chromatography.. *J Chromatogr A*. 19 (1), 3201-3216.